

Science with the Einstein Telescope: a comparison of different designs

Michele Maggiore & Marica Branchesi



1st ET Annual Meeting
EGO, 15-17 Nov 2022

Science with the Einstein Telescope: a comparison of different designs

Marica Branchesi,^{1,2} Michele Maggiore,^{3,4} David Alonso,⁵ Charles Badger,⁶ Biswajit Banerjee,^{1,2} Freija Beirnaert,⁷ Swetha Bhagwat,^{8,9} Marie-Anne Bizouard,¹⁰ Guillaume Boileau,^{11,10} Ssohrab Borhanian,¹² Man Leong Chan,¹³ Nelson Christensen,¹⁰ Giulia Cusin,^{14,3,4} Stefan L. Danilishin,^{15,16} Jerome Degallaix,¹⁷ Valerio De Luca,¹⁸ Arnab Dhani,¹⁹ Tim Dietrich,^{20,21} Ulyana Dupletsa,^{1,2} Stefano Foffa,^{3,4} Gabriele Franciolini,⁸ Andreas Freise,^{22,15} Gianluca Gemme,²³ Boris Goncharov,^{1,2} Archisman Ghosh,⁷ Francesca Gulminelli,²⁴ Ish Gupta,¹⁹ Pawan Kumar Gupta,^{15,25} Jan Harms,^{1,2} Nandini Hazra,^{1,2,26} Stefan Hild,^{15,16} Tanja Hinderer,²⁷ Ik Siong Heng,²⁸ Francesco Iacovelli,^{3,4} Justin Janquart,^{15,25} Kamiel Janssens,^{10,11} Alexander C. Jenkins,²⁹ Chinmay Kalaghatgi,^{15,25,30} Tjonnie G. F. Li,^{31,32} Yufeng Li,³³ Eleonora Loffredo,^{1,2} Elisa Maggio,²¹ Michele Mancarella,^{3,4,34,35} Michela Mapelli,^{36,37,38} Katarina Martinovic,⁶ Andrea Maselli,^{1,2} Patrick Meyers,³⁹ Chiranjib Mondal,²⁴ Niccolò Muttoni,^{3,4} Harsh Narola,^{15,25} Micaela Oertel,⁴⁰ Gor Oganesyan,^{1,2} Costantino Pacilio,^{8,34,35} Paolo Pani,⁸ Albino Perego,^{41,42} Carole Pérois,^{36,37,38} Mauro Pieroni,^{43,44} Anna Puecher,^{15,25} Tania Regimbau,⁴⁵ Angelo Ricciardone,^{46,36,37} Antonio Riotto,^{3,4} Samuele Ronchini,^{1,2} Mairi Sakellariadou,⁶ Anuradha Samajdar,²⁰ Filippo Santoliquido,^{36,37,38} B.S. Sathyaprakash,^{19,47,48} Chris Van Den Broeck,^{15,25} and Teng Zhang^{9,16}

Motivations

The reference ET configuration:

- triangle, 10km arms
- 3 nested detectors in xylophone configuration (HF+LF cryo)

We want to evaluate the effect on the Science Case of

- changes in geometry: triangle vs 2L, and different arm-lengths
- role of low-frequency instrument

why now and not 10 yr ago?

when the basic layout of ET was first proposed (<2011) and until very recently, there were not even the elements for performing such a study

- only after GWTC-3 (+ recent theoretical population modeling) we have enough info on the coalescing binaries (redshift, mass distributions,...), so to optimize the ET design
- many of the most interesting specific Sciences Cases for 3G detectors have been developed only in recent years, in the flurry of activities after the first detection
- thanks to the OSB, we now have the large ET theoretical community needed to perform such a study (50+ people involved)

now this study becomes possible and, therefore, mandatory

configurations studied

geometries:

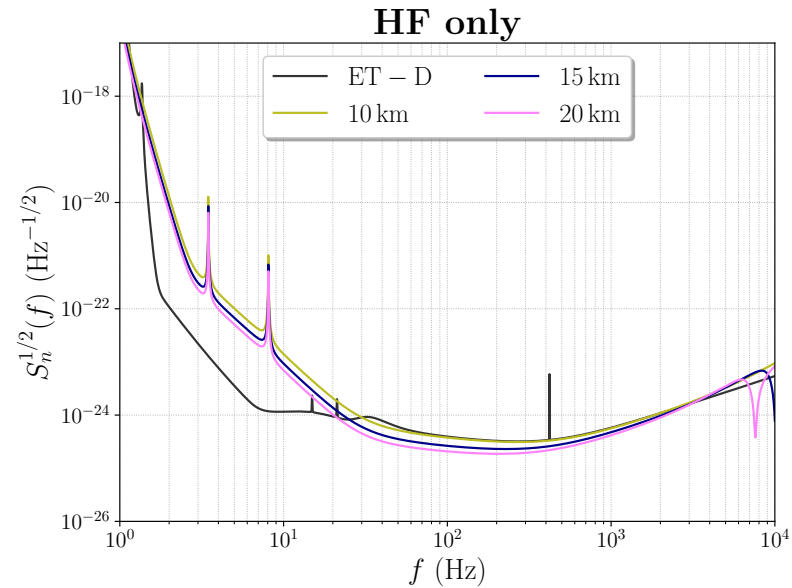
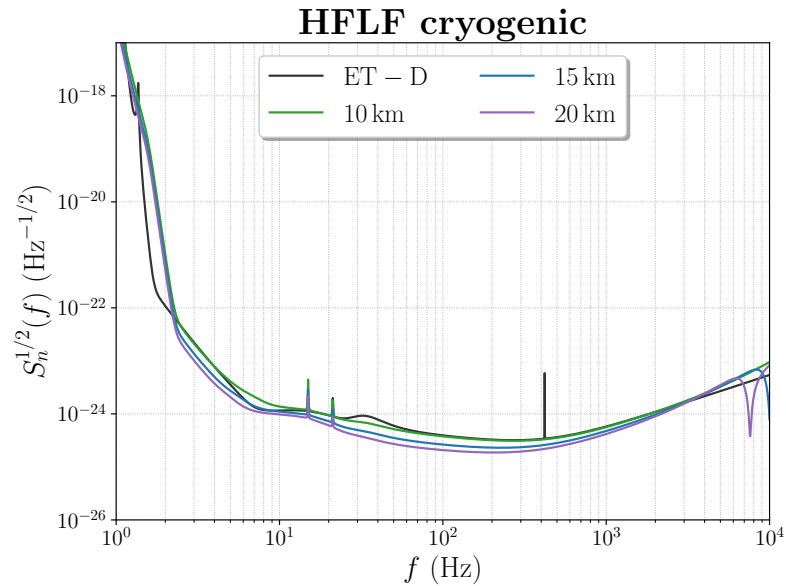
- triangle, 10km arms (the current baseline ET geometry)
- 2L, 15km arms, parallel
- 2L, 15km arms at 45°
- triangle, 15km arms
- 2L, 20km arms, parallel
- 2L, 20km arms at 45°

triangle-10km and 2L-15km
or
triangle-15km and 2L-20km

have comparable excavation volumes:
nested interferometers requires tunnels
with larger diameter (~ 8m vs 6.5m)
and more caverns

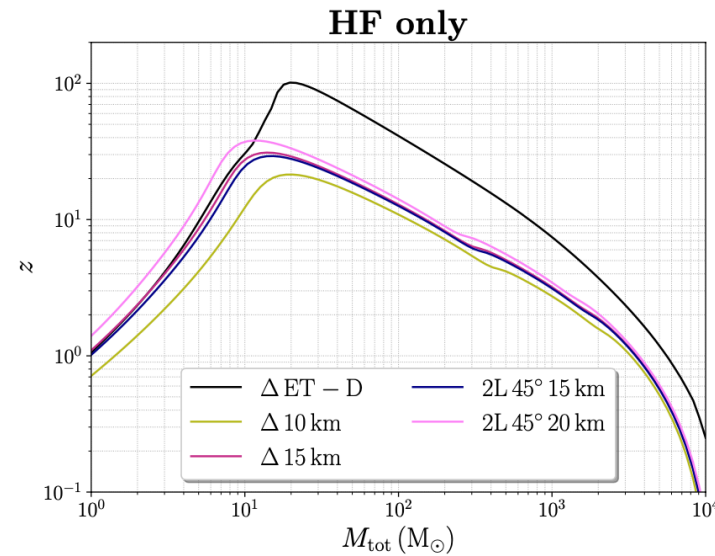
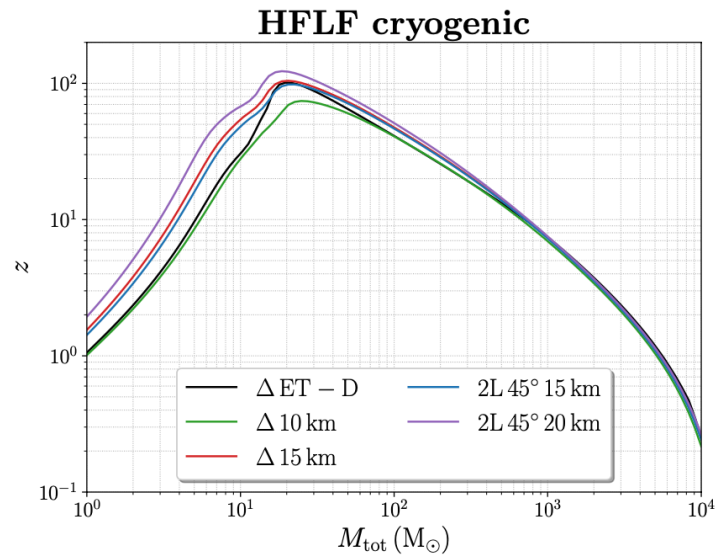
A detailed cost analysis need and well beyond
the scope of our work

amplitude spectral density (ASD)

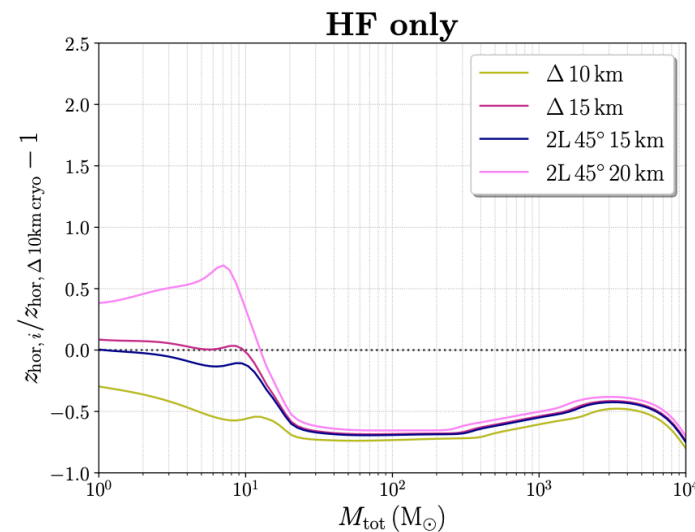
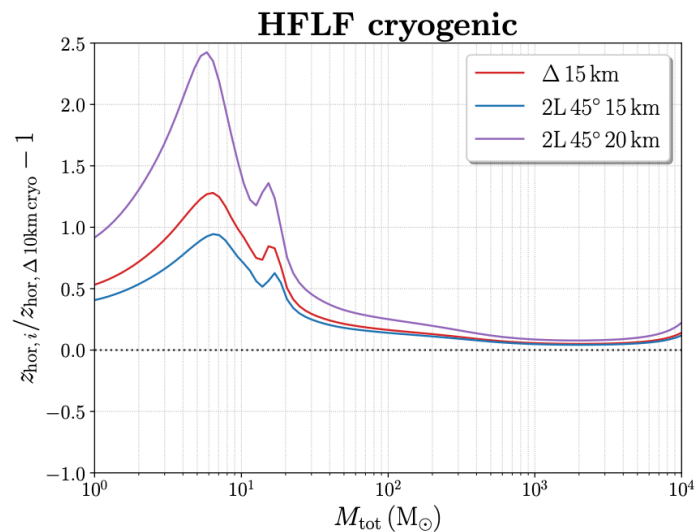


- full HFLF cryo, or HF instrument only
- sensitivity curves provided by the ISB
- the HFLF cryo curve used updates the ET-D curve.
- note: actual curves still evolving

horizon distance for equal mass binaries



horizon distances



relative differences in horizon, wrt the full (HFLF-cryo) 10km triangle

structure of the work

Contents

1 Introduction	1	6 Impacts of detector designs on specific science cases	60
2 Detector geometries and sensitivity curves	3	6.1 Physics near the BH horizon	60
3 Coalescence of compact binaries	7	6.1.1 Testing the GR predictions for space-time dynamics near the horizon	60
3.1 Binary Black Holes	8	6.1.2 Searching for echoes and near-horizon structures	64
3.2 Binary Neutron Stars	18	6.1.3 Constraining tidal effects and multipolar structure	65
3.3 ET in a network of 3G detectors	25	6.2 Nuclear physics	68
4 Multi-messenger astrophysics	30	6.2.1 Radius estimation from Fisher-matrix computation	68
4.1 BNS sky-localization and pre-merger alerts	30	6.2.2 Full parameter estimation results	71
4.2 Gamma-ray bursts: joint GW and high-energy detections	34	6.2.3 Connected uncertainty of nuclear-physics parameters	73
4.2.1 Prompt emission	34	6.2.4 Postmerger detectability	74
4.2.2 Afterglow: survey and pointing modes	36	6.2.5 Conclusions: nuclear physics with ET	76
4.3 Kilonovae: joint GW and optical detections	39	6.3 Population studies	76
5 Stochastic backgrounds	42	6.3.1 Merger rate reconstruction	76
5.1 Sensitivity to stochastic backgrounds	44	6.3.2 Constraints on PBHs from high-redshift mergers	78
5.1.1 Power-law integrated sensitivity	45	6.3.3 Other PBH signatures	82
5.1.2 Angular sensitivity	48	6.4 Cosmology	85
5.2 Astrophysical backgrounds	50	6.4.1 Hubble parameter and dark energy from joint GW/EM detections	85
5.3 Impact of correlated magnetic, seismic and Newtonian noise	53	6.4.2 Hubble parameter and dark energy from BNS tidal deformability	93
5.3.1 Seismic and Newtonian Noise	53	6.4.3 Hubble parameter from high-mass ratio events	96
5.3.2 Magnetic noise	56	6.4.4 Large Scale Structures from GWs	100
		6.5 Cosmological stochastic backgrounds	102
		6.5.1 Cosmic Strings	102
		6.5.2 Supercooled first-order phase transition	103
		6.5.3 Source separation	105
		7 The role of the null stream in the triangle-2L comparison	105
		8 Summary	108
		8.1 Comparison of different geometries	109
		8.2 The role of the low-frequency sensitivity	115
		8.3 Conclusions	119
		A Tables of figures of merit for BBHs and BNSs	121

coalescence of compact binaries

(BBH, BNS)

we study detection rates, range and distribution in redshift, accuracy in the reconstruction of the source parameters

very general metrics that already provide a first solid understanding

first step (lasted several months):

development and comparison of Fisher codes

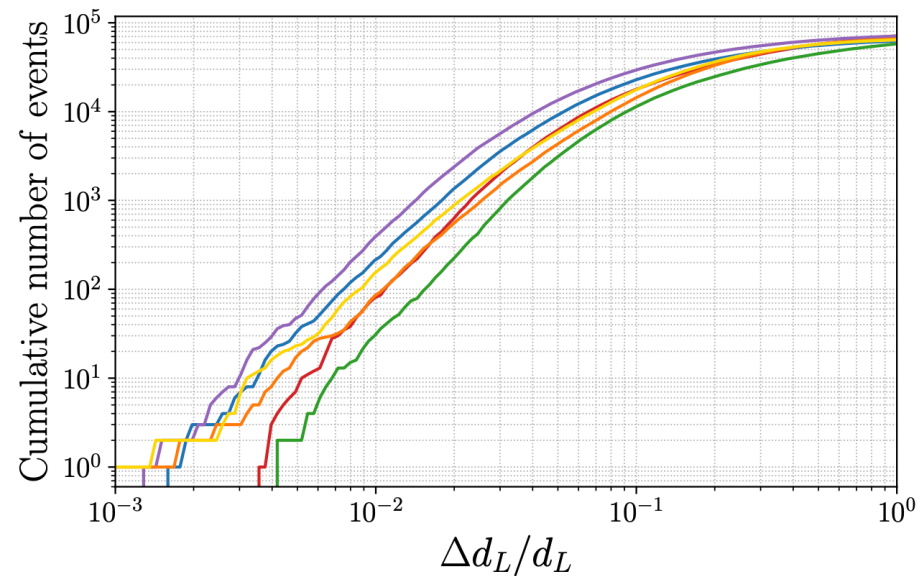
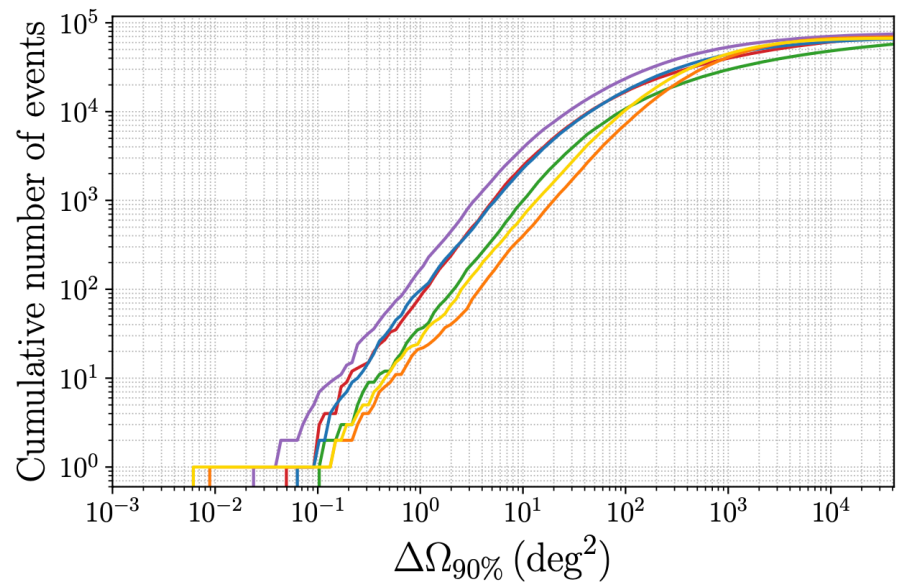
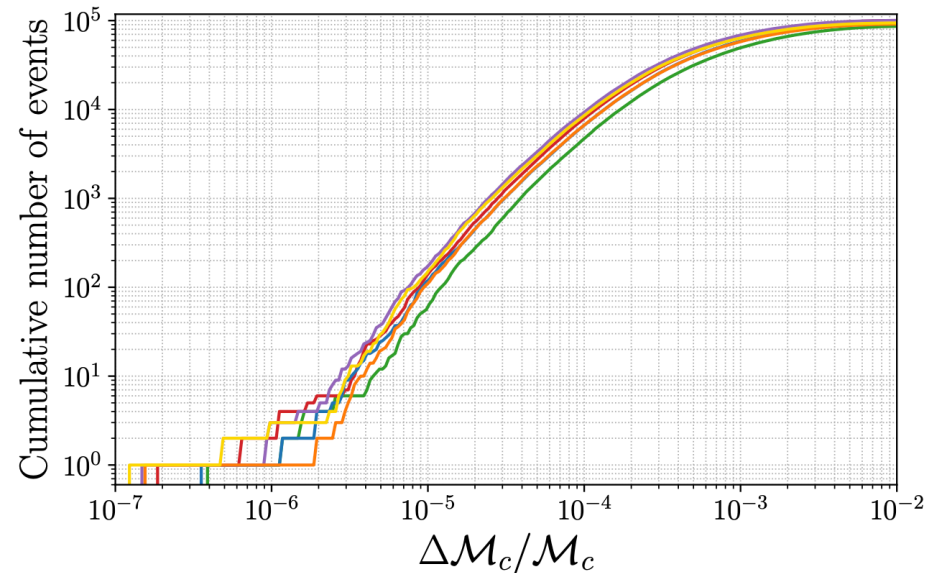
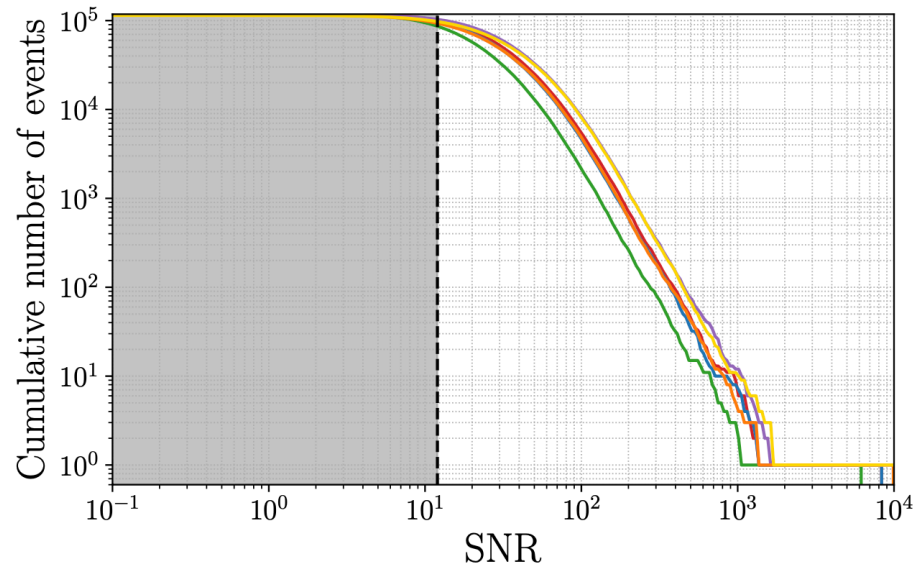
- GWBENCH (Borhanian 2021, Borhanian and Sathyaprakash 2022)
- GWFISH (Harms, Dupletsa et al 2022, Ronchini et al 2022, GSSI group)
- GWFAST (Iacovelli, Mancarella, Foffa, MM 2022, Geneva Group)
- TiDoFM (Li, Heng, Chan et al 2022)
- (Pieroni, Ricciardone, Barausse 2022)

other technical details:

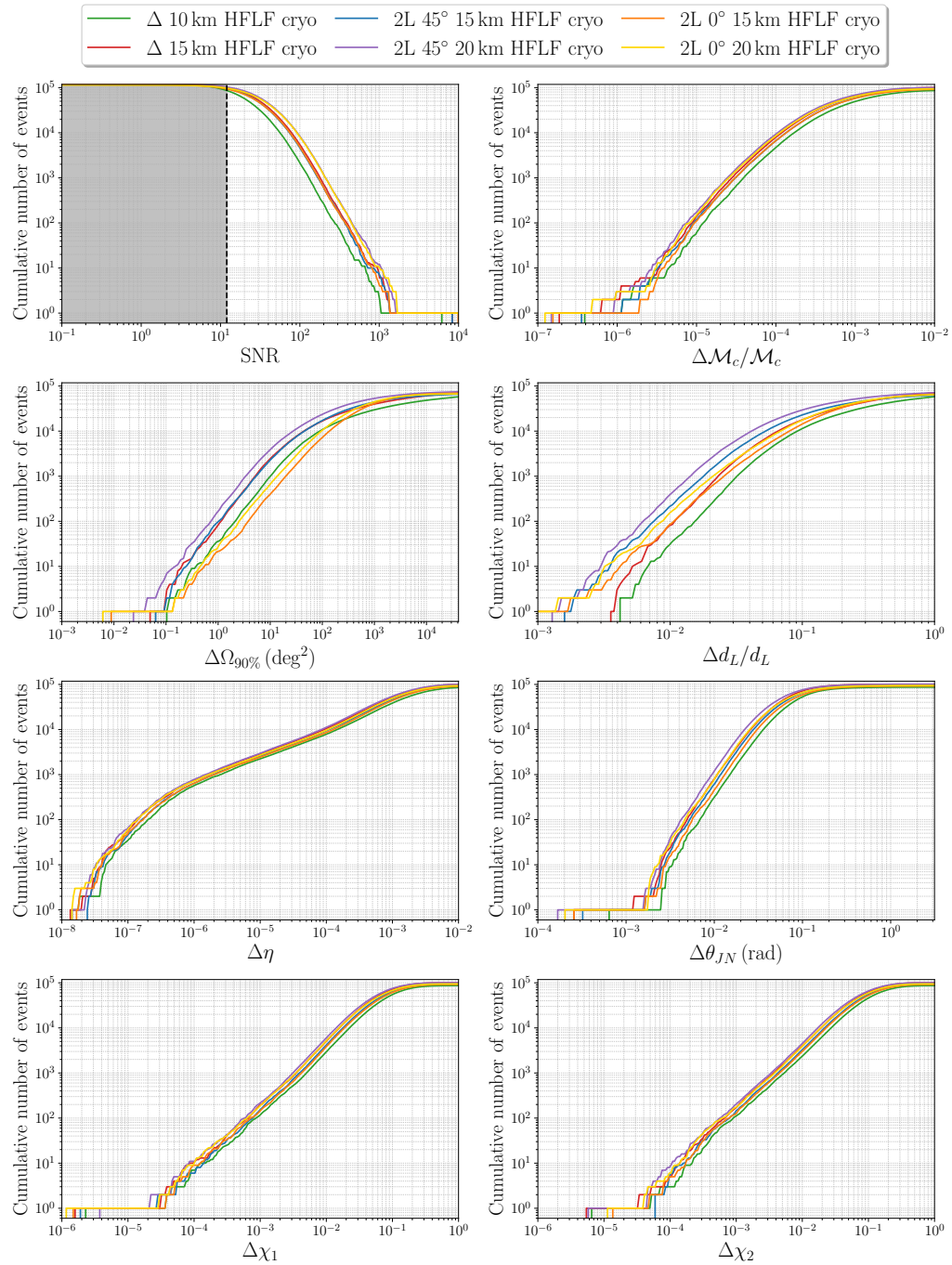
- state-of-the art population models (Santoliquido et al 2021)
- state-of-the art waveform models
 - IMRPhenomXPHM for BBHs (includes precessing spins and higher-order modes)
 - IMRPhenomD_NRTidalv2 for BNS (includes tidal effects)
- inference on a large parameter space

$$\{\mathcal{M}_c, \eta, d_L, \theta, \phi, \iota, \psi, t_c, \Phi_c, \chi_{1,x}, \chi_{2,x}, \chi_{1,y}, \chi_{2,y}, \chi_{1,z}, \chi_{2,z}, \Lambda_1, \Lambda_2\}$$

BBH



BBH



Configuration	SNR ≥ 8	SNR ≥ 12	SNR ≥ 50	SNR ≥ 100	SNR ≥ 200
Δ -10km-HFLF-Cryo	103 528	87 568	13 674	2298	282
Δ -15km-HFLF-Cryo	111 231	101 308	26 092	5730	759
2L-15km-45°-HFLF-Cryo	107 661	97 205	23 491	4933	644
2L-20km-45°-HFLF-Cryo	110 698	103 773	34 009	8828	1267
2L-15km-0°-HFLF-Cryo	104 935	94 015	24 088	5143	642
2L-20km-0°-HFLF-Cryo	106 417	98 274	32 915	8551	1246
LVK-O5	8603	2861	47	4	2

Configuration	$\Delta d_L/d_L \leq 0.1$	$\Delta d_L/d_L \leq 0.01$	$\Delta\Omega_{90\%} \leq 50 \text{ deg}^2$	$\Delta\Omega_{90\%} \leq 10 \text{ deg}^2$
Δ -10km-HFLF-Cryo	10 969	28	6064	914
Δ -15km-HFLF-Cryo	17 321	77	10 470	2273
2L-15km-45°-HFLF-Cryo	22 237	202	10 304	2124
2L-20km-45°-HFLF-Cryo	28 801	365	14 920	3648
2L-15km-0°-HFLF-Cryo	13 865	79	3030	374
2L-20km-0°-HFLF-Cryo	17 008	144	4706	608
LVK-O5	767	1	1607	599

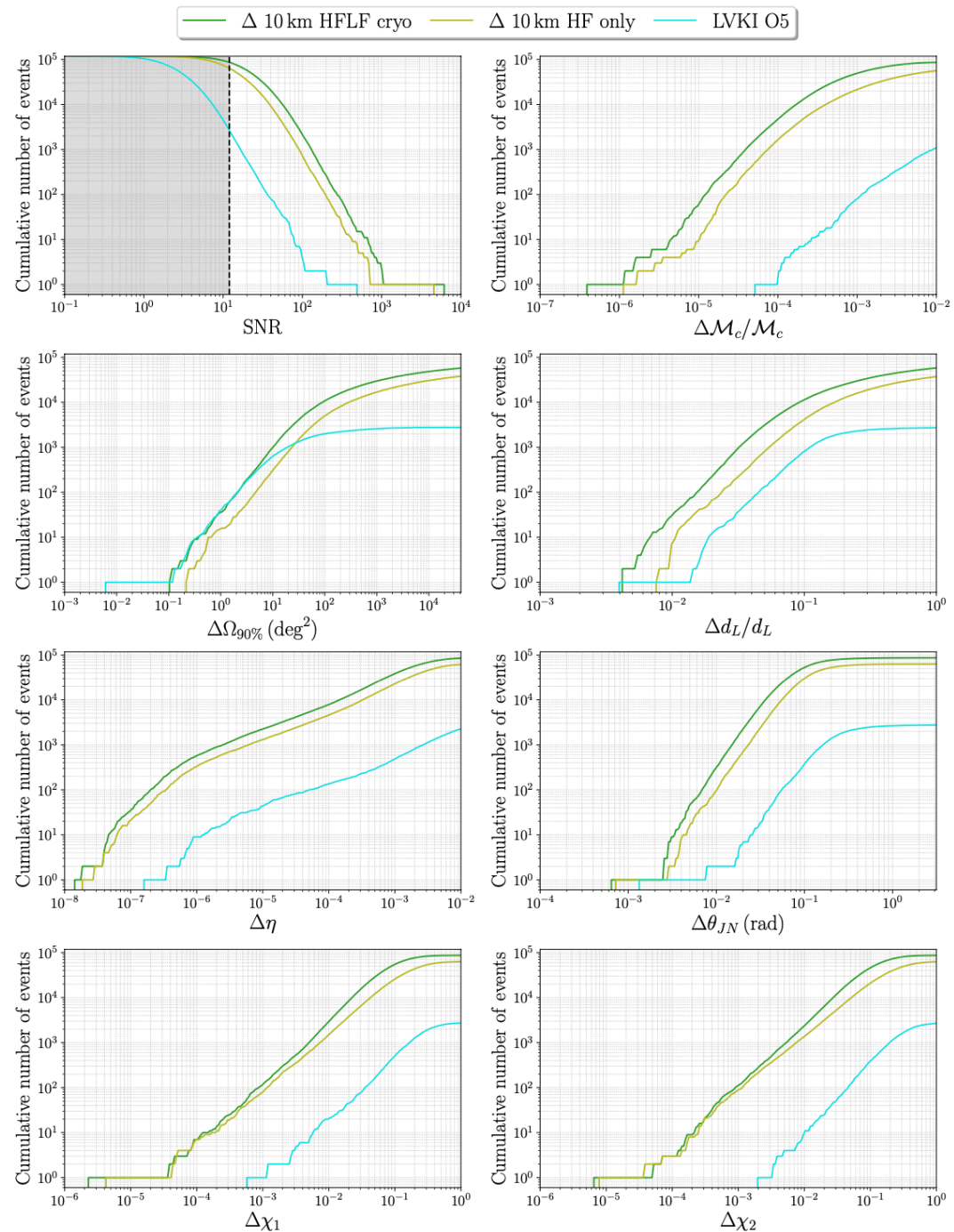
Configuration	$\Delta\mathcal{M}_c/\mathcal{M}_c \leq 10^{-3}$	$\Delta\mathcal{M}_c/\mathcal{M}_c \leq 10^{-4}$	$\Delta\chi_1 \leq 0.05$	$\Delta\chi_1 \leq 0.01$
Δ -10km-HFLF-Cryo	48 922	4549	27 877	2811
Δ -15km-HFLF-Cryo	64 469	7703	41 612	4856
2L-15km-45°-HFLF-Cryo	58 371	6456	35 943	3958
2L-20km-45°-HFLF-Cryo	67 999	9073	45 666	5706
2L-15km-0°-HFLF-Cryo	57 330	6472	33 236	3653
2L-20km-0°-HFLF-Cryo	63 154	8279	40 068	4935

- the baseline 10km triangle has, by itself, fantastic performances, improving by several orders of magnitudes on 2G detectors
- for BBH, the 2L-15km-45° improves significantly on the 10 km triangle for d_L and angular localization, and is slightly better (~ 2) for the other parameters

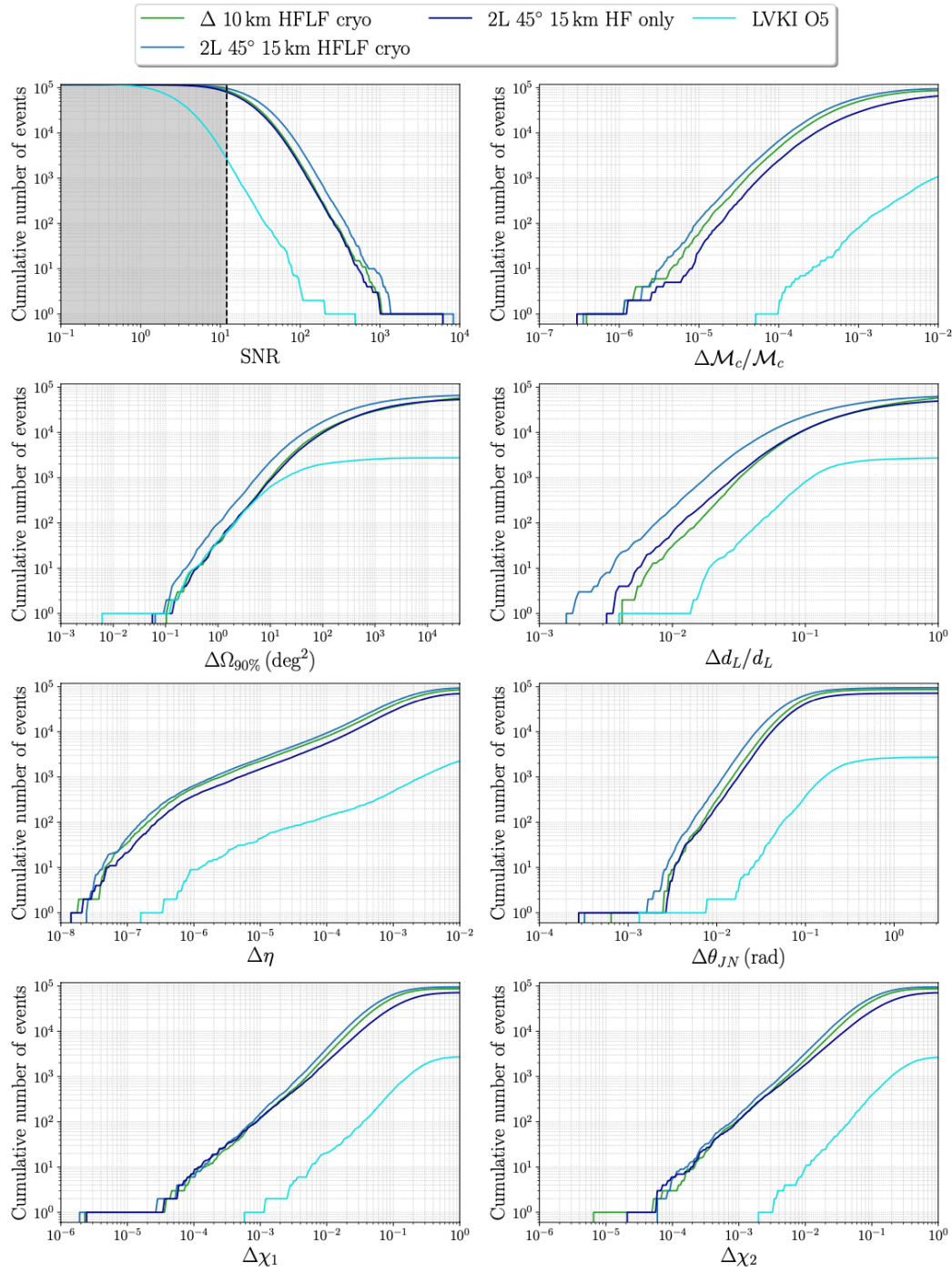
actually, 2L-15km-45° equal or better even than the 15 km triangle

- 2L with parallel arms quite disfavored, because of a comparatively poor angular localization capability

triangle 10-km well superior
to LVK-O5 even in HF-only
configuration
(except angular localization)



BBH

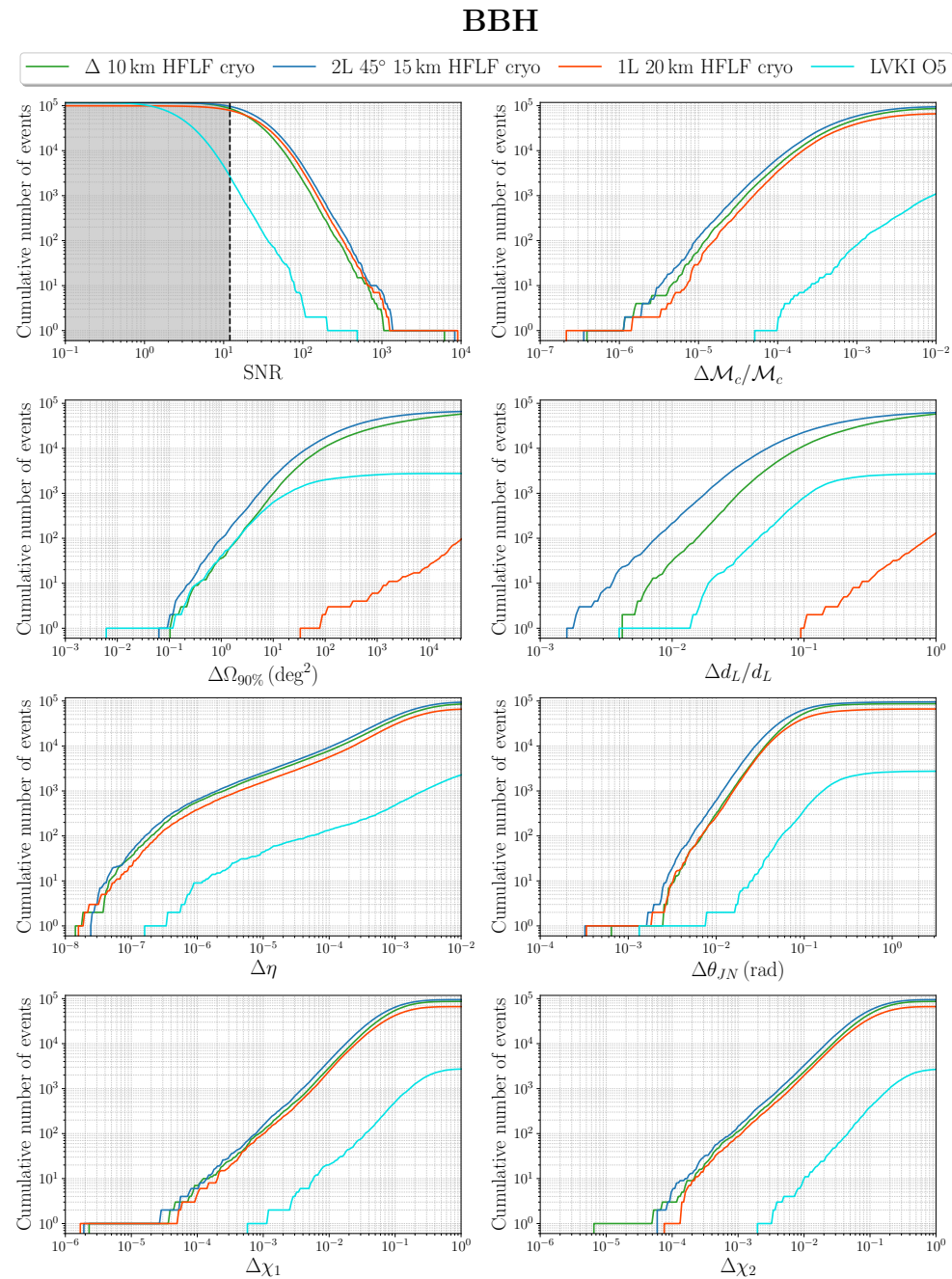


for BBH, the 2L-15km-45° HF-only is comparable or better than the 10km triangle at full sensitivity

Configuration	$\Delta d_L/d_L \leq 0.1$	$\Delta d_L/d_L \leq 0.01$	$\Delta\Omega_{90\%} \leq 50 \text{ deg}^2$	$\Delta\Omega_{90\%} \leq 10 \text{ deg}^2$
Δ -10km-HFLF-Cryo	10 969	28	6064	914
Δ -15km-HFLF-Cryo	17 321	77	10 470	2273
2L-15km-45°-HFLF-Cryo	22 237	202	10 304	2124
2L-20km-45°-HFLF-Cryo	28 801	365	14 920	3648
2L-15km-0°-HFLF-Cryo	13 865	79	3030	374
2L-20km-0°-HFLF-Cryo	17 008	144	4706	608
Δ -10km-HF	3919	6	2409	281
Δ -15km-HF	8083	26	5156	817
2L-15km-45°-HF	11 193	56	5263	835
2L-20km-45°-HF	16 155	113	8448	1566
2L-15km-0°-HF	4111	17	1054	120
2L-20km-0°-HF	9693	57	2936	362

a single L-shaped detector, not inserted in a global network, is basically useless for those aspects of the Science Case, such as multi-messenger astronomy or cosmology, that require accurate reconstruction of sky localization and distance of the sources

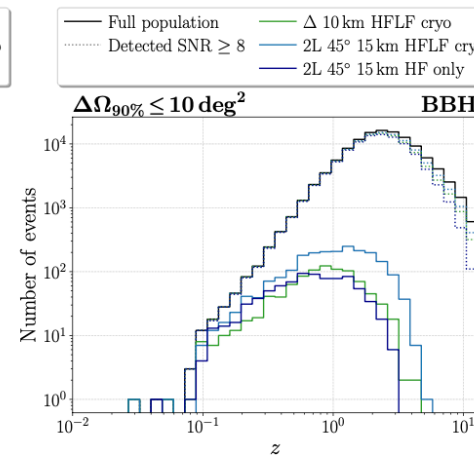
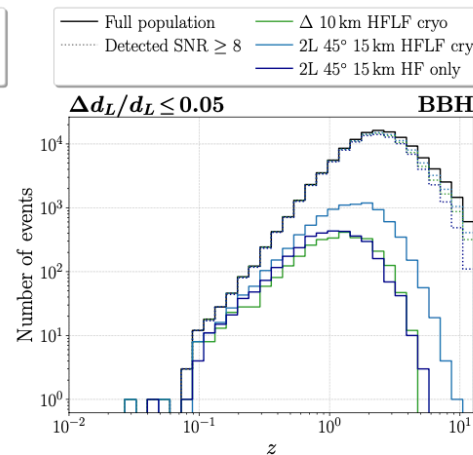
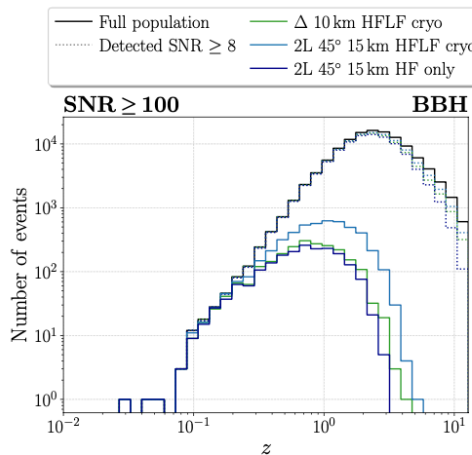
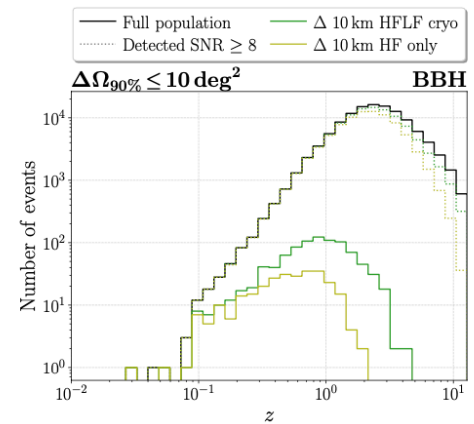
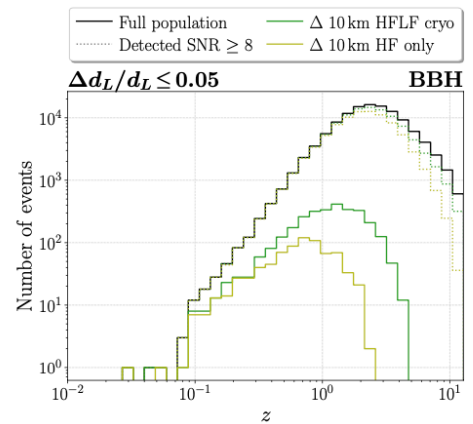
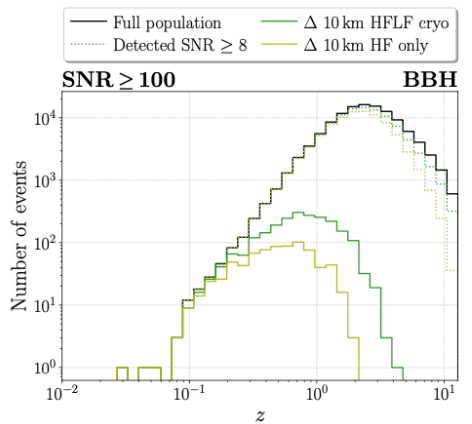
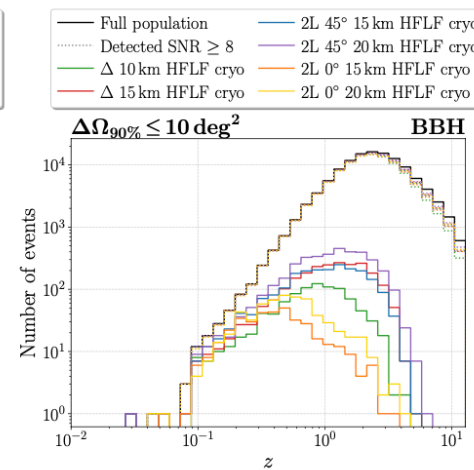
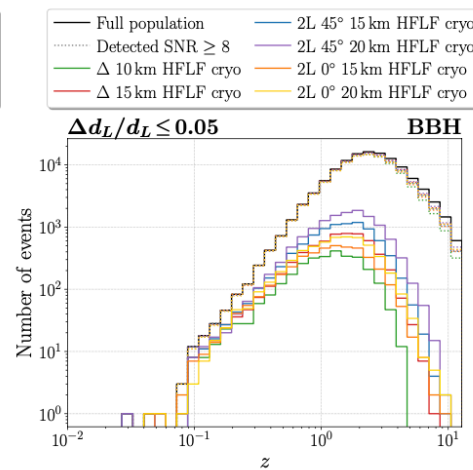
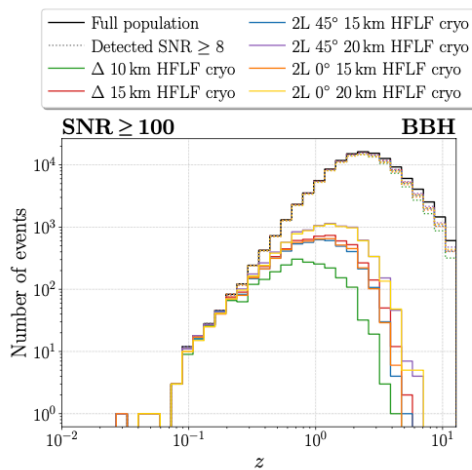
it is competitive on other parameters (assuming that glitches can be reliably vetoed)



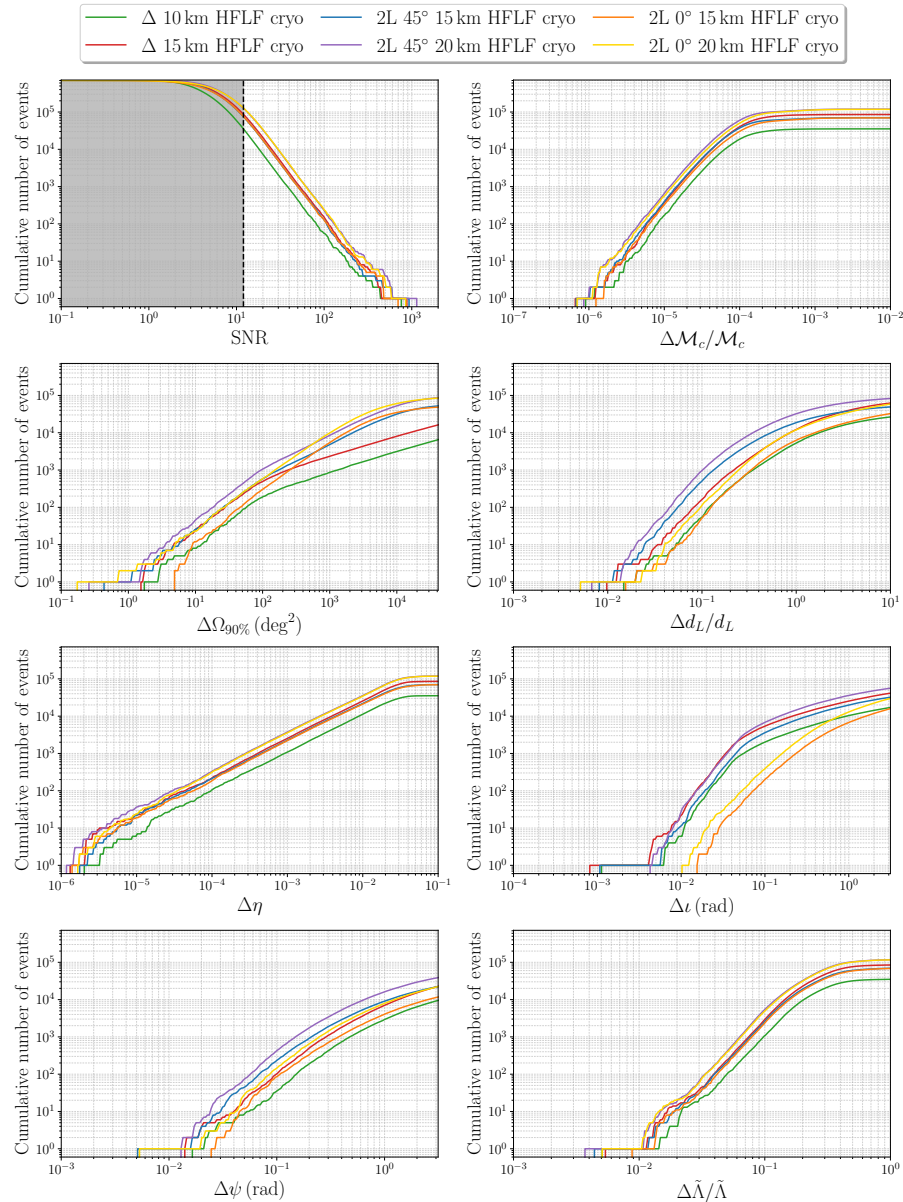
BBH 'golden' events

the 2L-45° and Δ -15km give the best compromise between detecting many of them, up to large redshift, and localizing them.

2L-15km-45°, even with HF-only, is comparable to Δ -10km with full HFLF-cryo sensitivity



BNS



BNS

confirms the basic message from BBHs

the baseline 10km triangle has remarkable performances, improving by orders of magnitude wrt 2G

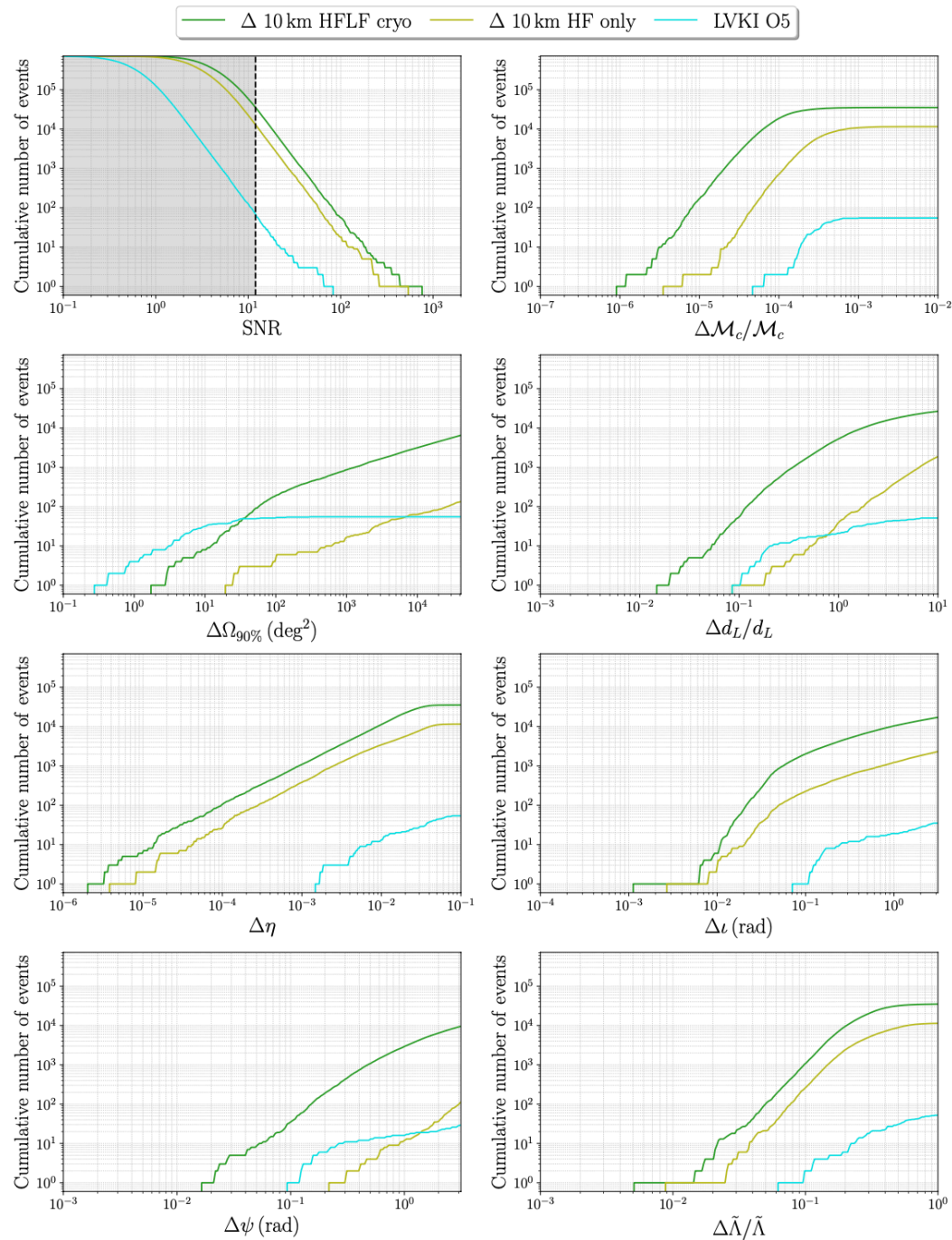
the 2L-15km-45° improves by a further factor 2-3

2L-15km-0° disfavored

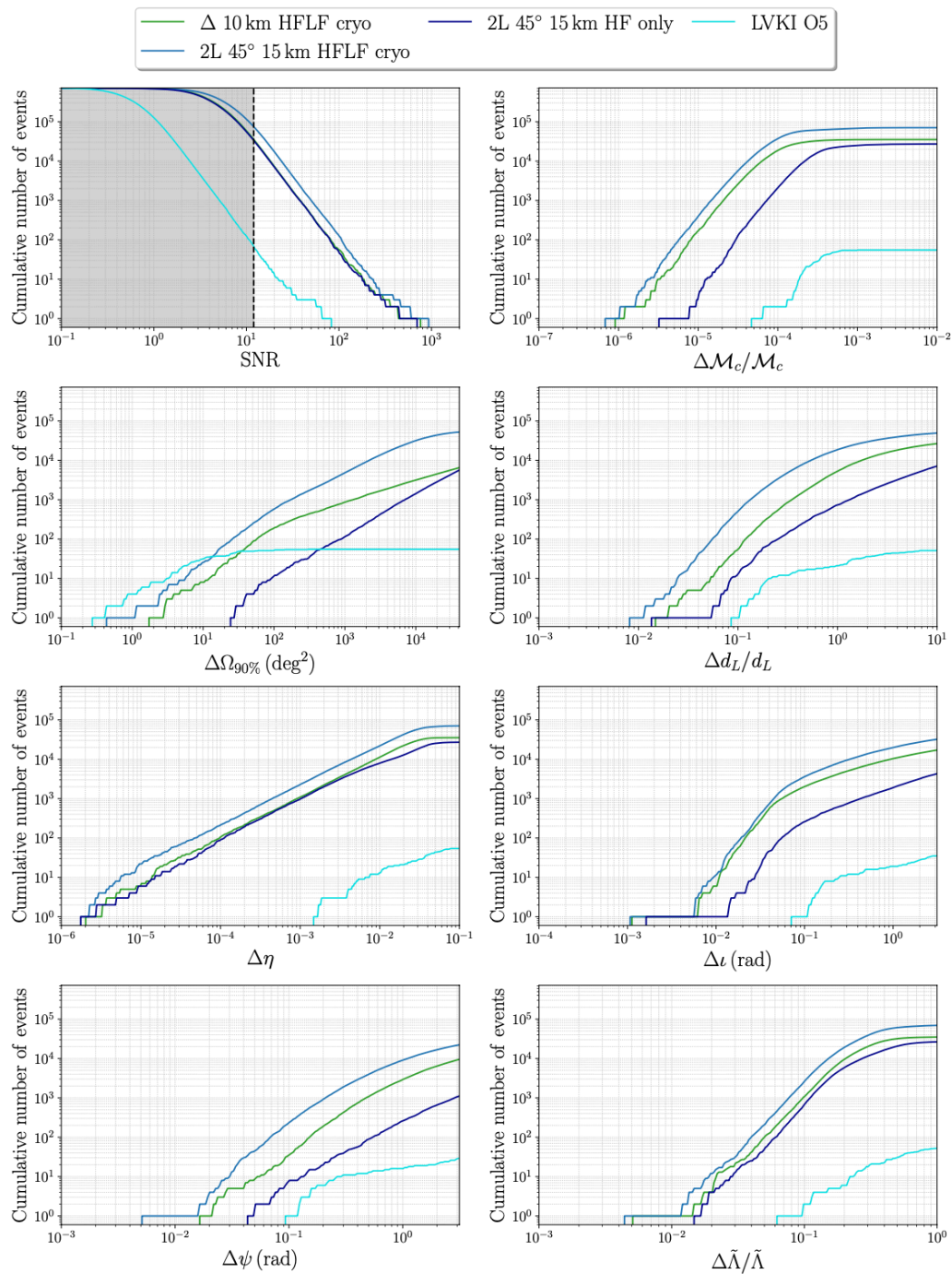
BNS

Losing the LF in the 10km triangle:

LF sensitivity particularly important
for BNS (long time in bandwidth)



BNS

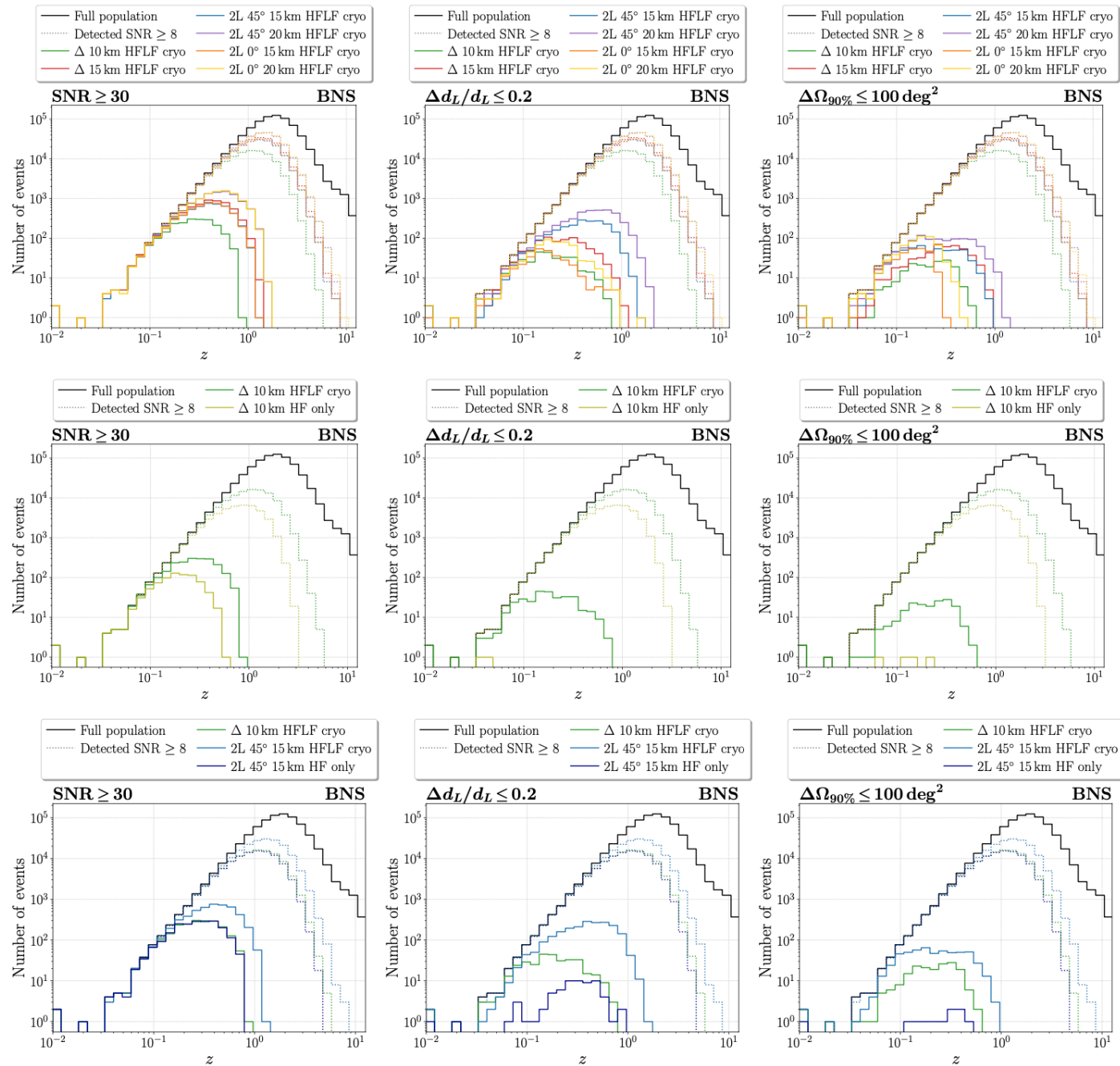


The 2L-15km-45° improves on the 10-km triangle

but now, 2L-15km-45° -HFonly sensibly worse than triangle 10km full HFLF-cryo

again, LF especially important for BNS

BNS 'golden' events



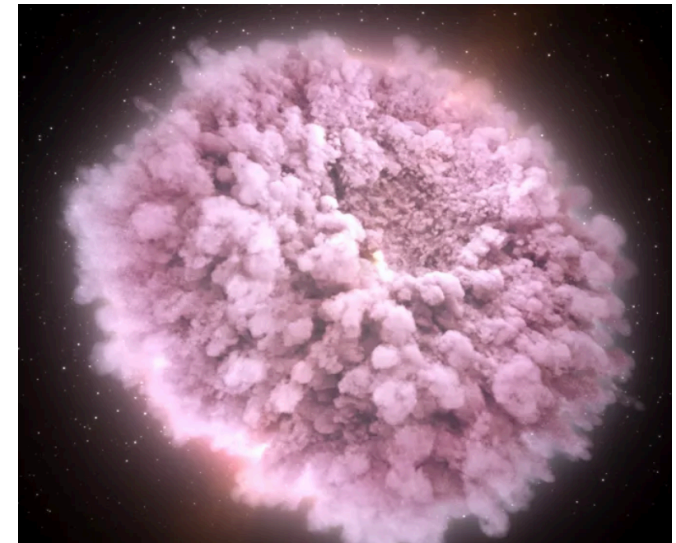
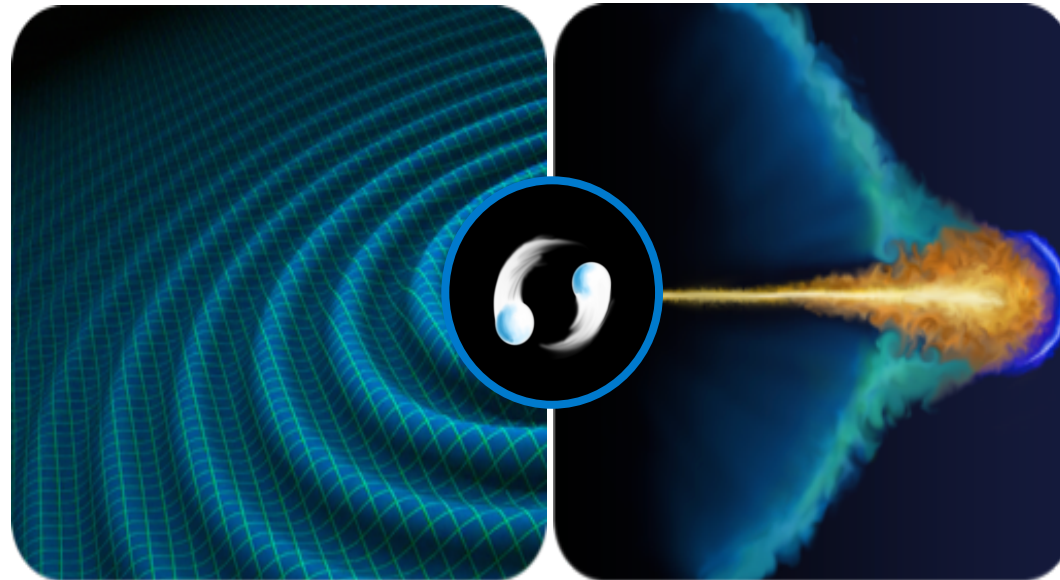
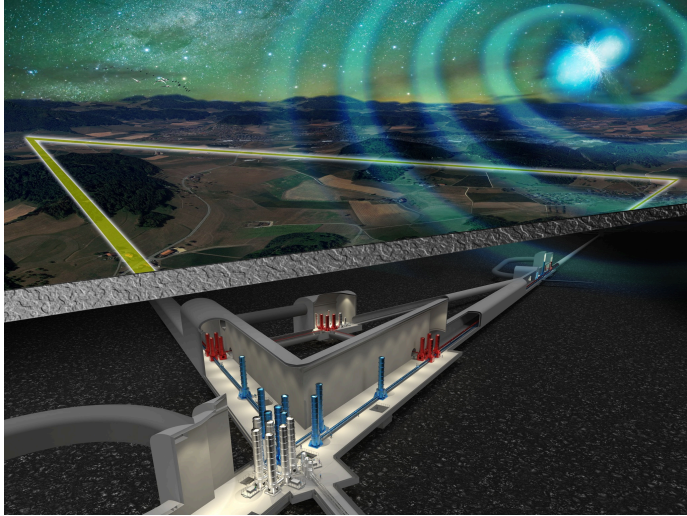
ET in a network with 1CE (40km) or 2CE (40km + 20km)

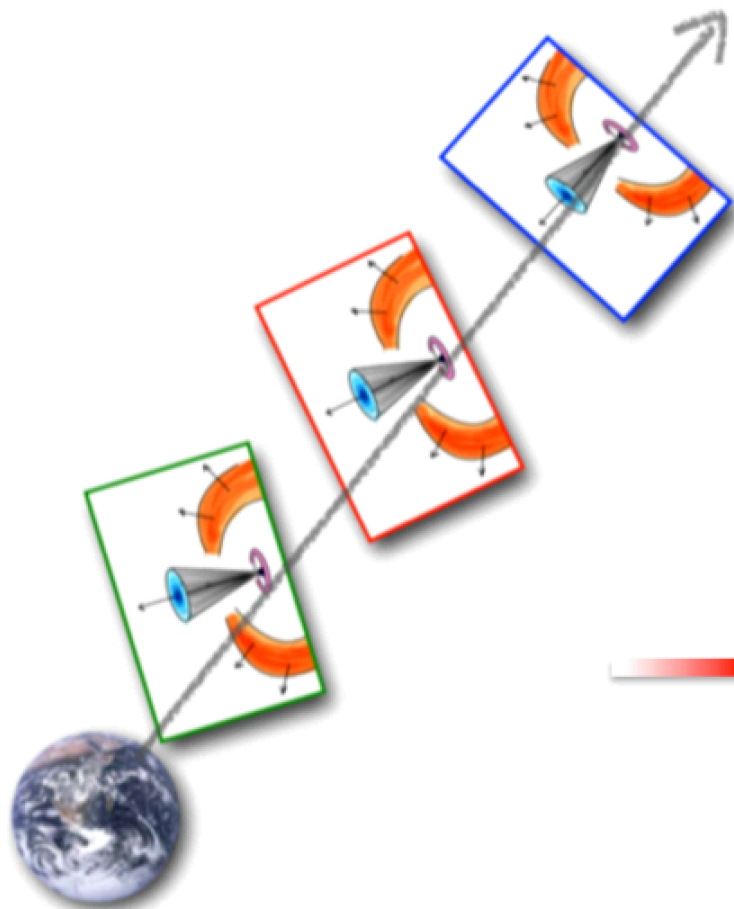
Configuration	$\Delta d_L/d_L \leq 0.3$	$\Delta d_L/d_L \leq 0.1$	$\Delta\Omega_{90\%} \leq 100 \text{ deg}^2$	$\Delta\Omega_{90\%} \leq 10 \text{ deg}^2$
Δ -10km-HFLF-Cryo+CE-40km	32 053	4100	54 994	2427
2L-15km-45°-HFLF-Cryo+CE-40km	45 252	7949	75 828	3838
2L-15km-0°-HFLF-Cryo+CE-40km	16 999	2079	29 821	1515
Δ -10km-HFLF-Cryo+2CE	72 335	13 630	112 705	6570
2L-15km-45°-HFLF-Cryo+2CE	89 877	19 129	145 272	9841
2L-15km-0°-HFLF-Cryo+2CE	78 798	14 909	125 640	7592

BNS

differences are smaller but still significant, especially with 1 CE

Multi-messenger Astrophysics with ET

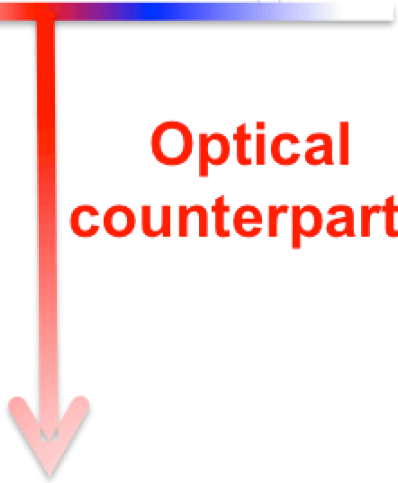




**High-energy
Counterparts**



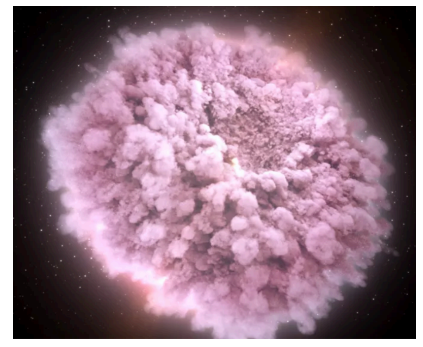
**Optical
counterparts**



RELATIVISTIC JET PHYSICS,
GRB EMISSION MECHANISMS,
COSMOLOGY and MODIFIED GRAVITY



KILONOVA PHYSICS,
NUCLEOSYNTHESIS, NUCLEAR
PHYSICS and H0 ESTIMATE



Credits: Ghirlanda



High-energy Counterparts

RELATIVISTIC JET PHYSICS,
GRB EMISSION MECHANISMS,
COSMOLOGY and MODIFIED GRAVITY



- NUMBER OF JOINT DETECTIONS
- REACHED REDSHIFT
- PARAMETER ESTIMATION

Optical counterparts

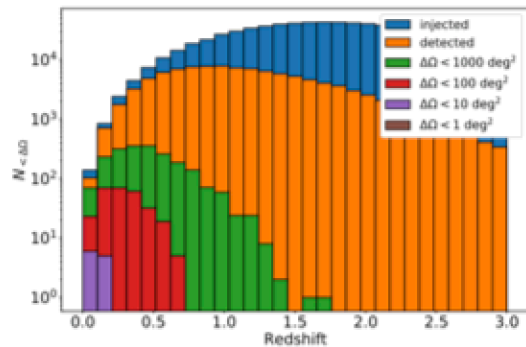
KILONOVA PHYSICS,
NUCLEOSYNTHESIS, NUCLEAR
PHYSICS and H_0 ESTIMATE



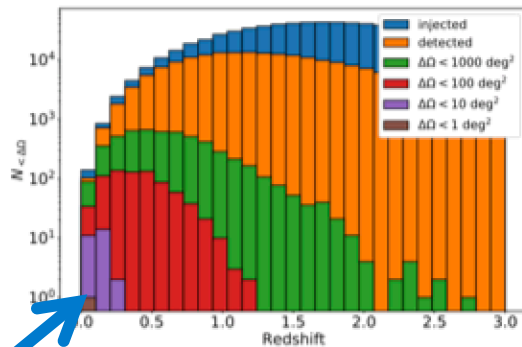
Key parameters:

- *Ability to localize the source*
- *Accessible Universe in terms of achieved z*
- *Pre-merger detection and PE*

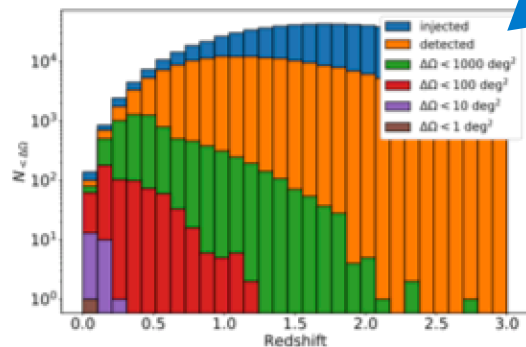
For the MM studies we use an SNR detection threshold of 8
We consider only 2L misaligned configurations



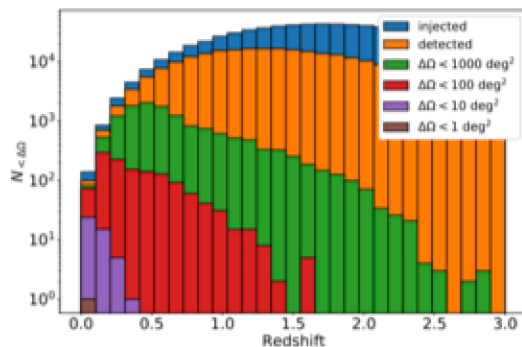
(a) Δ 10 km HFLF cryo



(b) Δ 15 km HFLF cryo



(d) 2L 15 km HFLF cryo



(e) 2L 20 km HFLF cryo

2L with 15 km misaligned arms

- comparable to 15 km triangle
- better than 10 km triangle

On-axis events

Full (HFLF cryo) sensitivity detectors

$\Delta\Omega_{90\%}(\text{deg}^2)$	All orientation BNSs				BNSs with viewing angle $\Theta_v < 15^\circ$			
	Δ 10	Δ 15	2L 15	2L 20	Δ 10	Δ 15	2L 15	2L 20
10	11	27	24	45	0	1	2	5
40	78	→	162	350	8	22	20	33
100	280	764	644	1282	26	74	68	133
1000	2112	5441	7478	13482	272	632	1045	1725

Factor 4 better

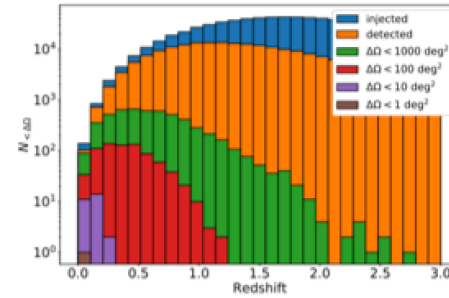
Without low-frequency

Full (HFLF cryo) sensitivity detectors

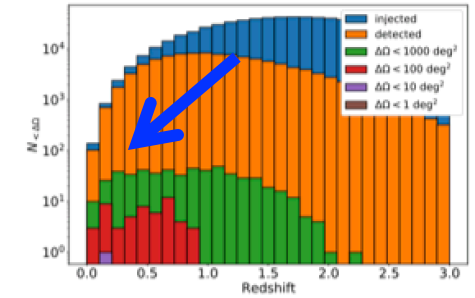
$\Delta\Omega_{90\%}(\text{deg}^2)$	All orientation BNSs				BNSs with viewing angle $\Theta_v < 15^\circ$			
	$\Delta 10$	$\Delta 15$	2L 15	2L 20	$\Delta 10$	$\Delta 15$	2L 15	2L 20
10	11	27	24	45	0	1	2	5
40	78	215	162	350	8	22	20	33
100	280	764	644	1282	26	74	68	133
1000	2112	5441	7478	13482	272	632	1045	1725

HF sensitivity detectors

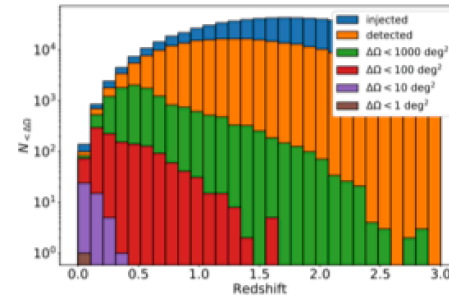
$\Delta\Omega_{90\%}(\text{deg}^2)$	All orientation BNSs				BNSs with viewing angle $\Theta_v < 15^\circ$			
	$\Delta 10$	$\Delta 15$	2L 15	2L 20	$\Delta 10$	$\Delta 15$	2L 15	2L 20
10	0	1	5	5	0	0	2	2
40	4	10	20	47	0	5	6	17
100	14	53	76	144	7	33	35	64
1000	145	548	1662	3378	80	336	672	1302



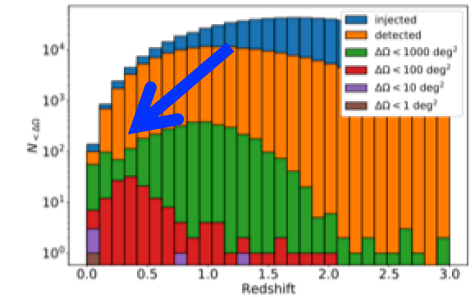
(b) $\Delta 15$ km HFLF cryo



(c) $\Delta 15$ km HF



(e) 2L 20 km HFLF cryo



(f) 2L 20 km HF

- significantly smaller number of well-localized events
- decrease of well-localized events more severe for the Δ configurations
- a large fraction of well-localized events already missed at small z
- on-axis events, decrease of well-localized events but in a smaller percentage than events randomly oriented

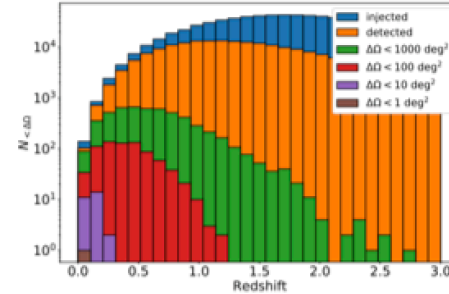
Without low-frequency

Full (HFLF cryo) sensitivity detectors

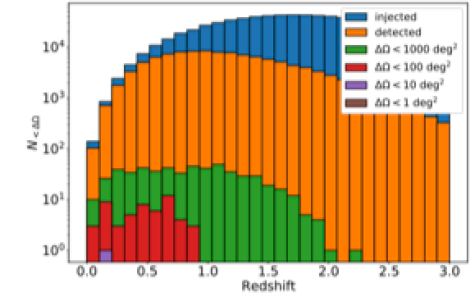
$\Delta\Omega_{90\%}(\text{deg}^2)$	All orientation BNSs				BNSs with viewing angle $\Theta_v < 15^\circ$			
	$\Delta 10$	$\Delta 15$	2L 15	2L 20	$\Delta 10$	$\Delta 15$	2L 15	2L 20
10	11	27	24	45	0	1	2	5
40	78	215	162	350	8	22	20	33
100	280	764	644	1282	26	74	68	133
1000	2112	5441	7478	13482	272	632	1045	1725

HF sensitivity detectors

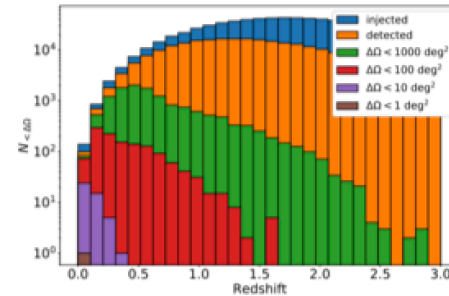
$\Delta\Omega_{90\%}(\text{deg}^2)$	All orientation BNSs				BNSs with viewing angle $\Theta_v < 15^\circ$			
	$\Delta 10$	$\Delta 15$	2L 15	2L 20	$\Delta 10$	$\Delta 15$	2L 15	2L 20
10	0	1	5	5	0	0	2	2
40	4	10	20	47	0	5	6	17
100	14	53	76	144	7	33	35	64
1000	145	548	1662	3378	80	336	672	1302



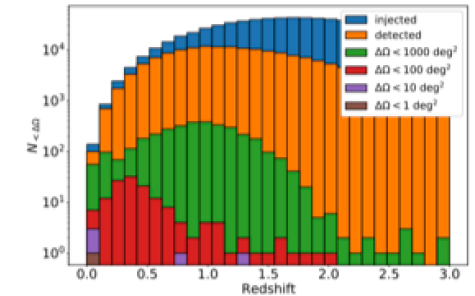
(b) $\Delta 15$ km HFLF cryo



(c) $\Delta 15$ km HF



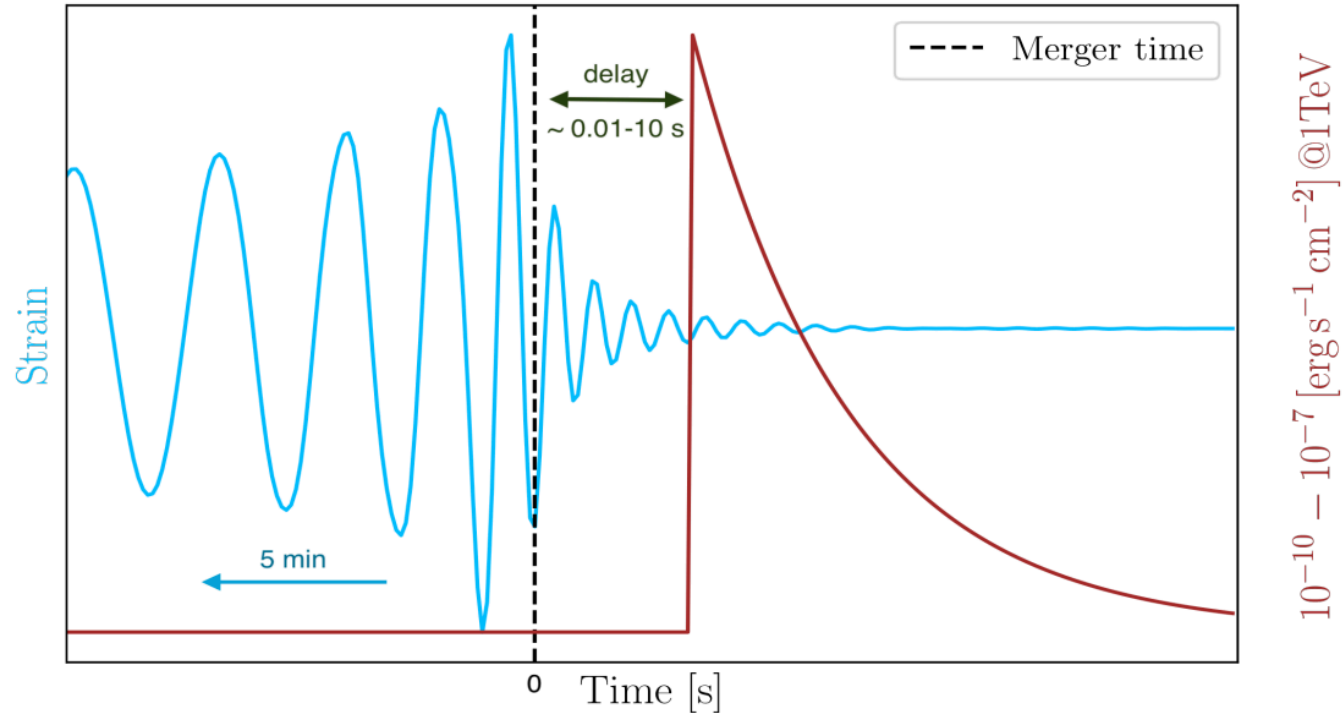
(e) 2L 20 km HFLF cryo



(f) 2L 20 km HF

- While HF 2L 15km and 2L20km localize worse than HFLF cryo $\Delta 10$ km **for randomly oriented systems**
- 2L HF15 km is comparable the full $\Delta 10$ km-cryo **for on-axis events**

Pre-merger detections



Credits: Banerjee et al. in prep

Critical to detect the prompt/early multi-wavelength emission

- to probe the central engine of GRBs, particularly to understand the jet composition, the particle acceleration mechanism, the radiation and energy dissipation mechanisms (e.g. VHE prompt CTA/ET synergy)
- to probe the structure of the outer sub-relativistic ejecta, early UV emission (e.g. ULTRASAT/UVEX/DORADO synergy)



Full (HFLF cryo) sensitivity detectors

Configuration	$\Delta\Omega_{90\%}$	All orientation BNSs			BNSs with $\Theta_v < 15^\circ$		
	[deg ²]	30 min	10 min	1 min	30 min	10 min	1 min
$\Delta 10\text{km}$	10	0	1	5	0	0	0
	100	10	39	113	2	8	20
	1000	85	293	819	10	34	10
	All detected	905	4343	23597	81	393	2312
$\Delta 15\text{km}$	10	1	5	11	0	1	1
	100	41	109	281	6	14	36
	1000	279	806	2007	33	102	295
	All detected	2489	11303	48127	221	1009	4024
2L 15 km misaligned	10	0	1	8	0	0	0
	100	20	54	169	2	7	26
	1000	194	565	1399	23	73	199
	All detected	2172	9598	39499	198	863	3432
2L 20 km misaligned	10	2	4	15	1	1	2
	100	39	118	288	7	19	47
	1000	403	1040	2427	47	128	346
	All detected	4125	17294	56611	363	1588	4377

$\Delta 15\text{km}$

- perform better than $\Delta 10\text{km}$ and 2L15km
- comparable to 2L20 km

Detections within $z=1.5$



Full (HFLF cryo) sensitivity detectors

Configuration	$\Delta\Omega_{90\%}$	All orientation BNSs			BNSs with $\Theta_v < 15^\circ$		
	[deg ²]	30 min	10 min	1 min	30 min	10 min	1 min
$\Delta 10\text{km}$	10	0	1	5	0	0	0
	100	10	39	113	2	8	20
	1000	85	293	819	10	34	10
	All detected	905	4343	23597	81	393	2312
$\Delta 15\text{km}$	10	1	5	11	0	1	1
	100	41	109	281	6	14	36
	1000	279	806	2007	33	102	295
	All detected	2489	11303	48127	221	1009	4024
2L 15 km misaligned	10	0	1	8	0	0	0
	100	20	54	169	2	7	26
	1000	194	565	1399	23	73	199
	All detected	2172	9598	39499	198	863	3432
2L 20 km misaligned	10	2	4	15	1	1	2
	100	39	118	288	7	19	47
	1000	403	1040	2427	47	128	346
	All detected	4125	17294	56611	363	1588	4377

2L15km better than $\Delta 10\text{km}$

Detections within $z=1.5$

On-axis similar

Without low-frequency



HF sensitivity detectors

Configuration	$\Delta\Omega_{90\%}$	All orientation BNSs			BNSs with $\Theta_v < 15^\circ$		
	[deg ²]	30 min	10 min	1 min	30 min	10 min	1 min
$\Delta 10\text{km}$	100	0	0	0	0	0	0
	1000	0	0	0	0	0	1
	All detected	0	0	0	0	0	26
$\Delta 15\text{km}$	100	0	0	0	0	0	0
	1000	0	0	0	0	0	4
	All detected	0	0	891	0	0	84
2L 15 km misaligned	100	0	0	0	0	0	0
	1000	0	0	7	0	0	3
	All detected	0	7	743	0	1	69
2L 20 km misaligned	100	0	0	3	0	0	0
	1000	0	0	13	0	0	6
	All detected	2	11	1535	0	1	146

NO localized pre-merger detections!

Detections within $z=1.5$

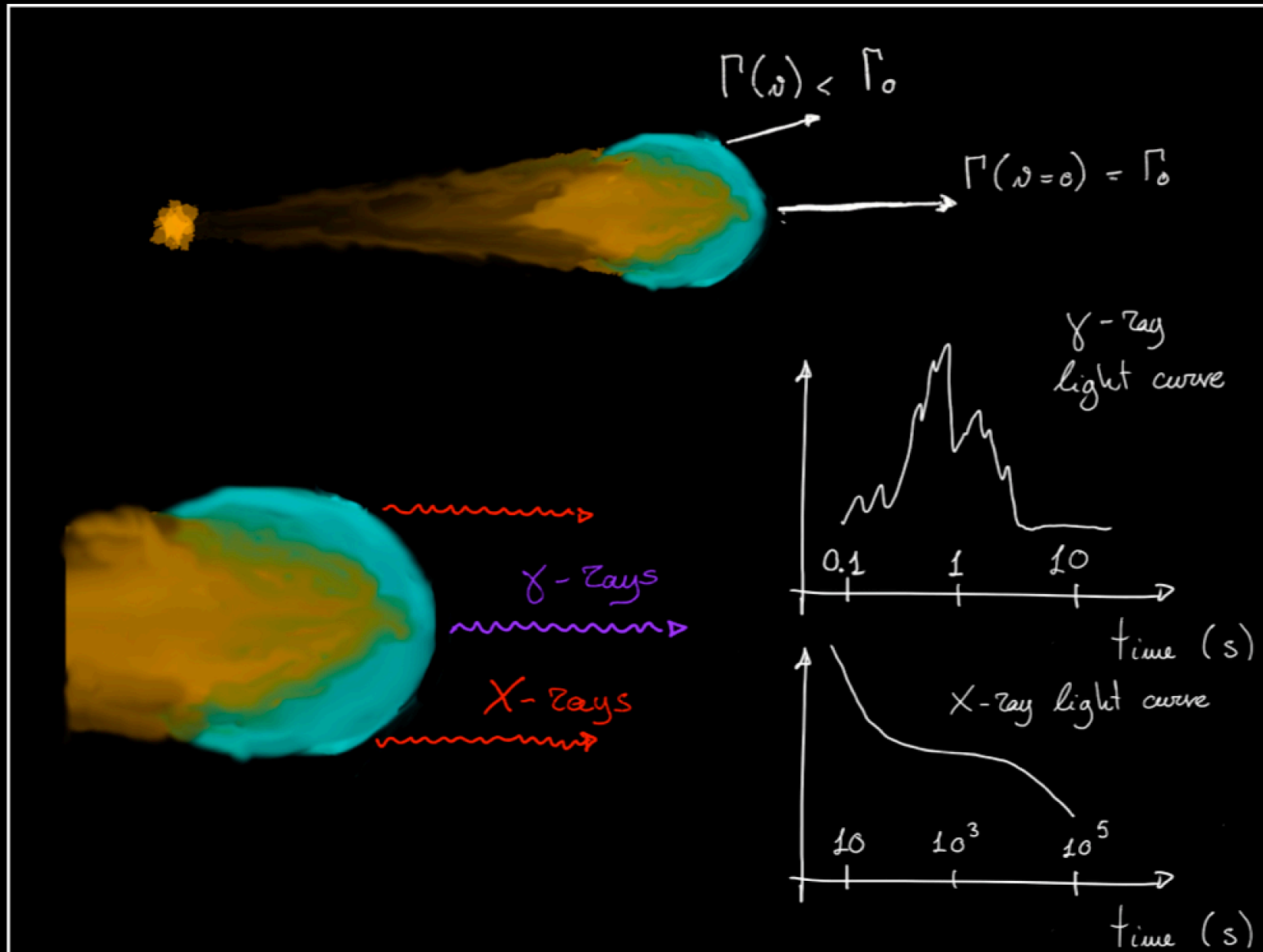
DRAMATIC DECREASE of pre-merger alerts!

HIGH-ENERGY

RELATIVISTIC JET PHYSICS,
GRB EMISSION MECHANISMS,
COSMOLOGY and MODIFIED GRAVITY

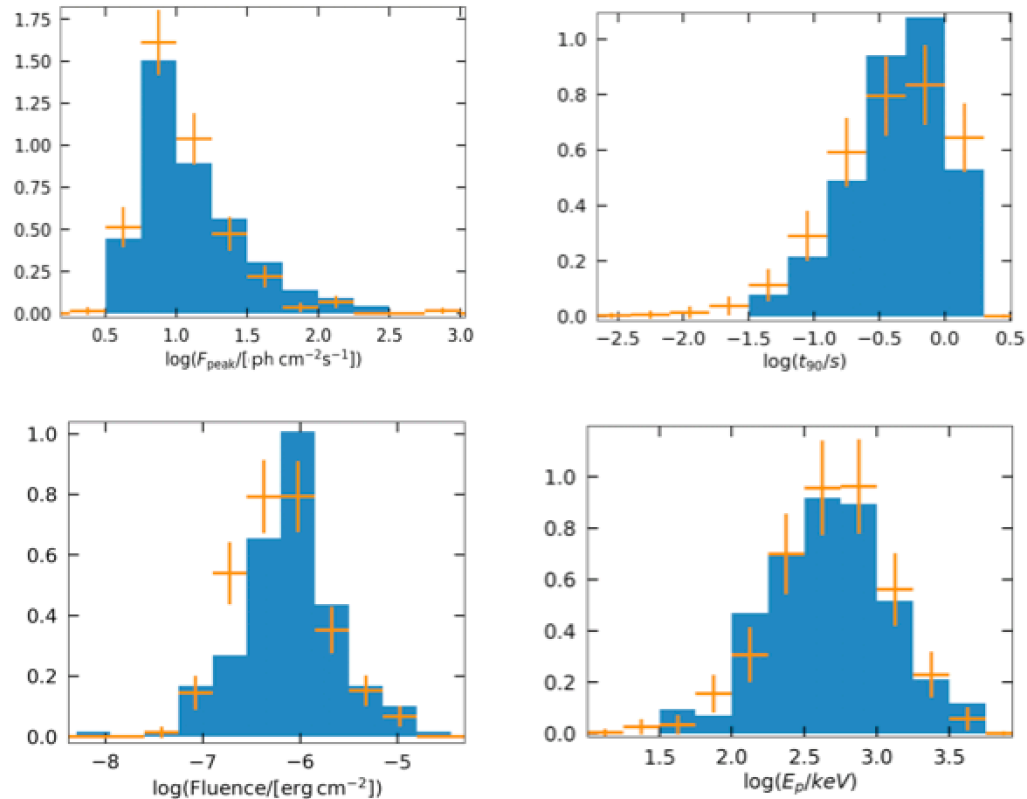
COSMOLOGY and MODIFIED GRAVITY

Prompt and afterglow emission from a structured jet



Model calibration using the properties of observed short GRB samples

- Starting with the BNS population
- Comparison with statistical properties of Fermi GBM short GRB sample
- Optimal parameters estimated via MCMC



$$\mathcal{R}_{SGRB} = f_{(NS-NS)\rightarrow jet} \times \mathcal{R}_{(NS-NS)}$$

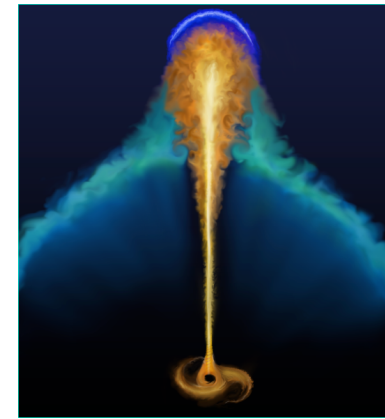
$0.26^{+0.34}_{-0.14}$

Rate of SGRB
observed by Fermi

From population
synthesis

GW + γ -ray joint detections per year

Survey mode



INSTRUMENT	band MeV	F_{lim} erg cm ⁻² s ⁻¹	FOV/4 π	loc. acc.	Status
<i>Fermi</i> -GBM	0.01 - 25	0.5	0.75	5 deg	Operating mission
GECAM	0.006 - 5	2×10^{-8}	1.0	1 deg	Operating mission
HERMES	0.05 - 0.3	0.2(*)	1.0	1 deg	Concept next few yrs
GRINTA-TED	0.02-10				Concept 2031
THESEUS					Concept 2037

A large percentage of short GRB will have a GW counterpart detected by ET!

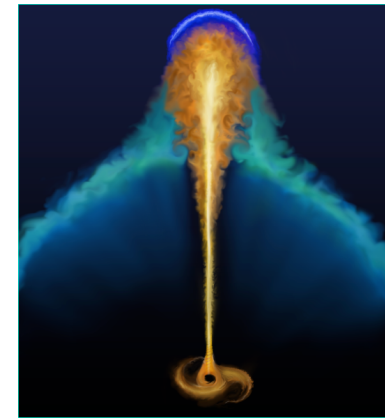
Instrument				$\Delta 10$	$\Delta 15$	2L 15	2L 20	
Fermi-GBM	59 ⁺¹¹ ₋₉	44 ⁺¹³ ₋₁₁	61 ⁺¹² ₋₁₁ %	83 ⁺⁹ ₋₁₀ %	79 ⁺⁸ ₋₁₁ %	89 ⁺⁴ ₋₈ %		
GECAM	89 ⁺⁵⁴ ₋₃₄	81 ⁺⁵¹ ₋₃₂	51 ⁺⁵ ₋₆ %	74 ⁺⁵ ₋₅ %	70 ⁺³ ₋₆ %	80 ⁺⁴ ₋₄ %		
HERMES	86 ⁺³¹ ₋₂₈	120 ⁺⁴⁰ ₋₃₁	117 ⁺³⁷ ₋₃₄	132 ⁺³⁴ ₋₃₄	55 ⁺⁹ ₋₇ %	78 ⁺⁸ ₋₇ %	74 ⁺⁹ ₋₉ %	85 ⁺⁵ ₋₆ %
GRINTA-TED	77 ⁺³¹ ₋₂₅	107 ⁺³¹ ₋₂₈	98 ⁺³¹ ₋₂₅	114 ⁺³⁴ ₋₂₈	57 ⁺¹⁰ ₋₉ %	79 ⁺⁸ ₋₈ %	74 ⁺⁹ ₋₉ %	85 ⁺⁵ ₋₅ %
THESEUS-XGIS	10 ⁺³ ₋₃	13 ⁺³ ₋₃	13 ⁺³ ₋₃	15 ⁺³ ₋₄	57 ⁺⁹ ₋₁₀ %	79 ⁺⁸ ₋₉ %	73 ⁺¹¹ ₋₇ %	85 ⁺⁷ ₋₅ %

Number of joint GW/GRB detections per year

Percentage of detected GRB with a GW signals

GW + γ -ray joint detections per year

Survey mode



INSTRUMENT	band MeV	F_{lim} erg cm ⁻² s ⁻¹	FOV/ 4π	loc. acc.	Status
<i>Fermi</i> -GBM	0.01 - 25	0.5	0.75	5 deg	Operating mission
GECAM	0.006 - 5	2×10^{-8}	1.0	1 deg	Operating mission
HERMES	0.05 - 0.3	0.2(*)	1.0	1 deg	Mission concept Pathfinder next few yrs
GRINTA-TED	0.02-10	0.45	0.64	5 deg(**)	Mission concept Launch 2031
THESEUS-XGIS	0.002 - 10	3×10^{-8}	0.16	< 15 arcmin	Mission concept Launch 2037

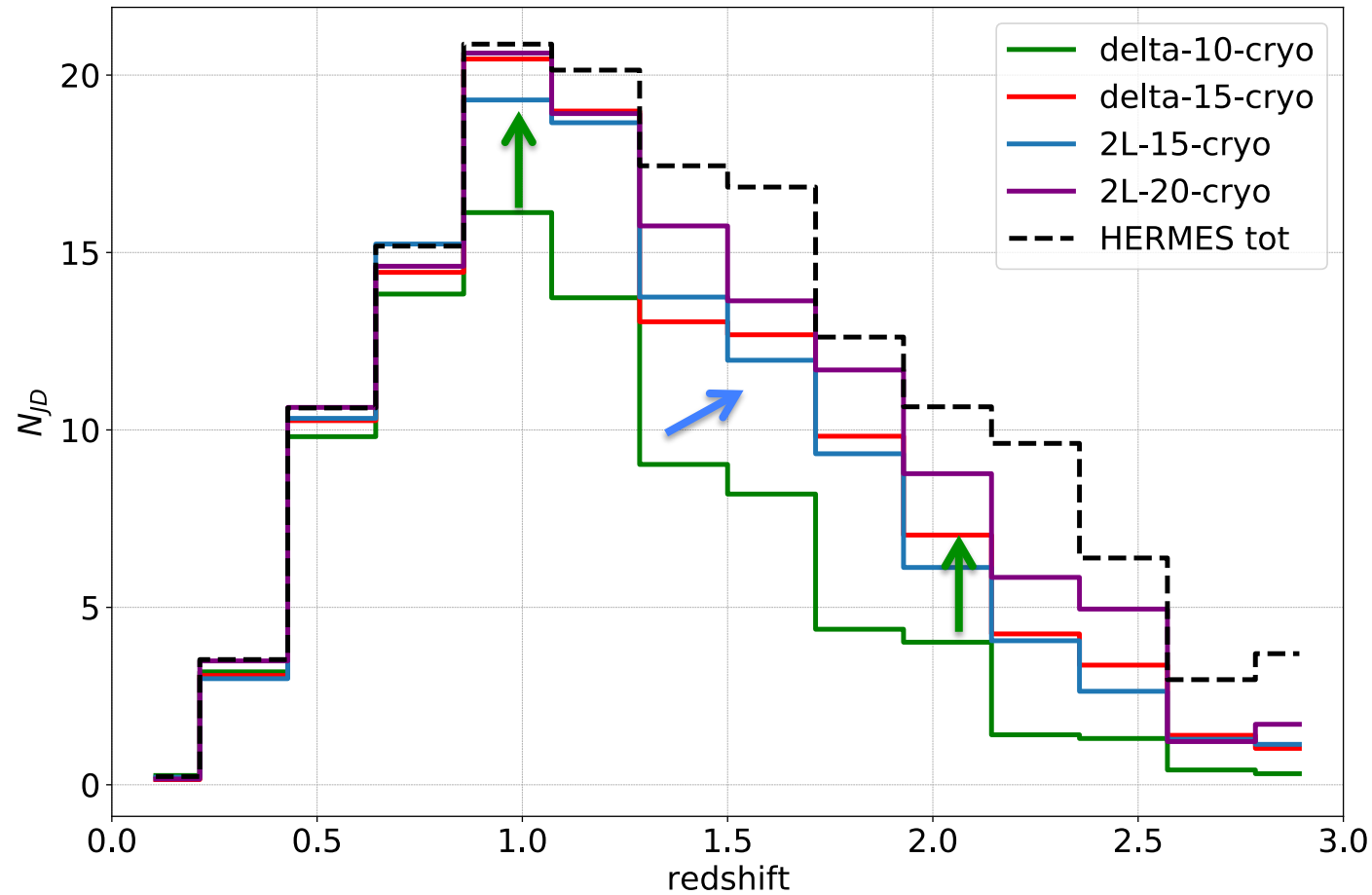
Full (HFLF cryo) sensitivity detectors

Instrument	$\Delta 10$	$\Delta 15$	2L 15	2L 20	$\Delta 10$	$\Delta 15$	2L 15	2L 20
Fermi-GBM	31 ⁺⁹ ₋₉	42 ⁺¹¹ ₋₁₃	39 ⁺¹¹ ₋₉	44 ⁺¹³ ₋₁₁	61 ⁺¹² ₋₁₁ %	83 ⁺⁹ ₋₁₀ %	79 ⁺⁸ ₋₁₁ %	89 ⁺⁴ ₋₈ %
GECAM	61 ⁺³⁹ ₋₂₅	89 ⁺⁵⁴ ₋₃₄	81 ⁺⁵¹ ₋₃₂	96 ⁺⁵² ₋₃₆	51 ⁺⁵ ₋₆ %	74 ⁺⁵ ₋₅ %	70 ⁺³ ₋₆ %	80 ⁺⁴ ₋₄ %
HERMES	86 ⁺³¹ ₋₂₈	120 ⁺⁴⁰ ₋₃₁	117 ⁺³⁷ ₋₃₄	132 ⁺³⁴ ₋₃₄	55 ⁺⁹ ₋₇ %	78 ⁺⁸ ₋₇ %	74 ⁺⁹ ₋₉ %	85 ⁺⁵ ₋₆ %
GRINTA-TED	77 ⁺³¹ ₋₂₅	107 ⁺³¹ ₋₂₈	98 ⁺³¹ ₋₂₅	114 ⁺³⁴ ₋₂₈	57 ⁺¹⁰ ₋₉ %	79 ⁺⁸ ₋₈ %	74 ⁺⁹ ₋₉ %	85 ⁺⁵ ₋₅ %
THESEUS-XGIS	10 ⁺³ ₋₃	13 ⁺³ ₋₃	13 ⁺³ ₋₃	15 ⁺³ ₋₄	57 ⁺⁹ ₋₁₀ %	79 ⁺⁸ ₋₉ %	73 ⁺¹¹ ₋₇ %	85 ⁺⁷ ₋₅ %



The percentage of GRBs with a GW counterpart significantly increases going from $\Delta 10$ km to 15 km and 20 km configurations

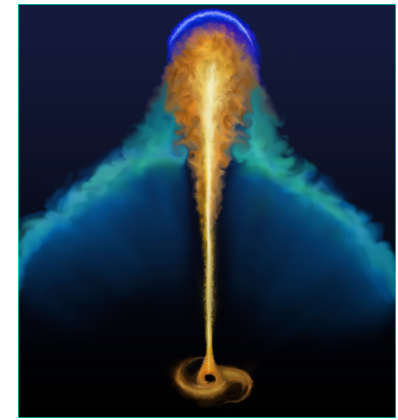
GW + γ -ray joint detections during one year for HERMES



- the most significant improvement is from $\Delta 10$ km to a 15 km configuration
- 15 and 20 km configurations are able to increase the number of joint detections at $z > 0.9$ with respect to $\Delta 10$ km (cosmological parameter and test of modified gravity)

GW + γ -ray joint detections per year

Survey mode



Full (HFLF cryo) sensitivity detectors

Instrument	$\Delta 10$	$\Delta 15$	2L 15	2L 20	$\Delta 10$	$\Delta 15$	2L 15	2L 20
Fermi-GBM	31^{+9}_{-9}	42^{+11}_{-13}	39^{+11}_{-9}	44^{+13}_{-11}	$61^{+12}_{-11}\%$	$83^{+9}_{-10}\%$	$79^{+8}_{-11}\%$	$89^{+4}_{-8}\%$
GECAM	61^{+39}_{-25}	89^{+54}_{-34}	81^{+51}_{-32}	96^{+52}_{-36}	$51^{+5}_{-6}\%$	$74^{+5}_{-5}\%$	$70^{+3}_{-6}\%$	$80^{+4}_{-4}\%$
HERMES	86^{+31}_{-28}	120^{+40}_{-31}	117^{+37}_{-34}	132^{+34}_{-34}	$55^{+9}_{-7}\%$	$78^{+8}_{-7}\%$	$74^{+9}_{-9}\%$	$85^{+5}_{-6}\%$
GRINTA-TED	77^{+31}_{-25}	107^{+31}_{-28}	98^{+31}_{-25}	114^{+31}_{-25}				
THESEUS-XGIS	10^{+3}_{-3}	13^{+3}_{-3}	13^{+3}_{-3}	15^{+3}_{-4}				

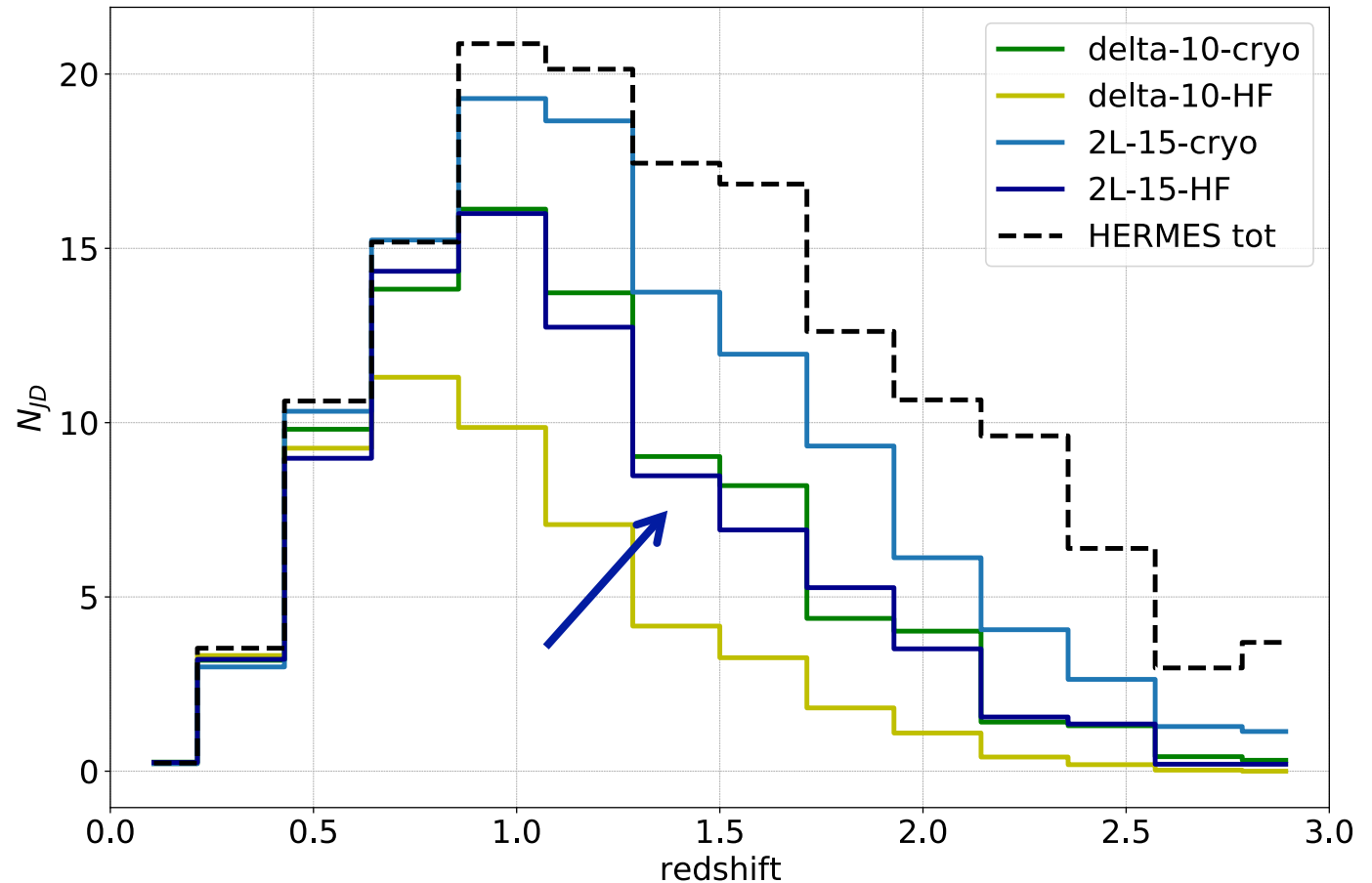
↓

HF sensitivity detectors

Instrument	$\Delta 10$	$\Delta 15$	2L 15	2L 20
Fermi-GBM	20^{+8}_{-7}	33^{+9}_{-9}	29^{+11}_{-9}	38^{+12}_{-10}
GECAM	35^{+21}_{-15}	62^{+38}_{-22}	58^{+38}_{-22}	77^{+47}_{-30}
HERMES	52^{+21}_{-18}	91^{+30}_{-29}	83^{+28}_{-28}	107^{+40}_{-31}
GRINTA-TED	46^{+22}_{-16}	80^{+31}_{-25}	74^{+28}_{-25}	94^{+33}_{-23}
THESEUS-XGIS	6^{+2}_{-2}	10^{+3}_{-3}	9^{+3}_{-3}	12^{+3}_{-3}

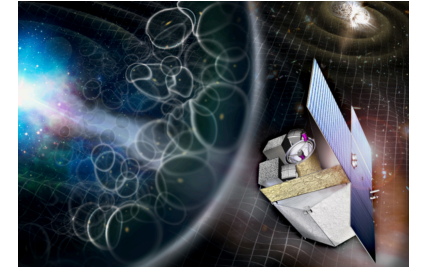
HF only:

- percentage of detected short GRBs w significantly decreases for each configu
- the performance of $\Delta 15$ km and 2L15 comparable to $\Delta 10$ km full sensitivity



Joint detection GW+X-ray afterglow per year

SURVEY MODE



THESEUS

Full (HFLF cryo) sensitivity detectors

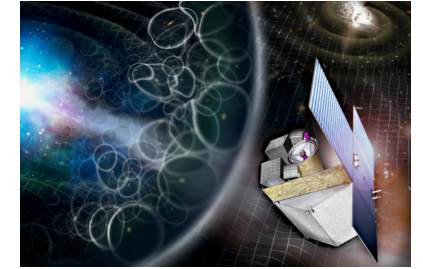
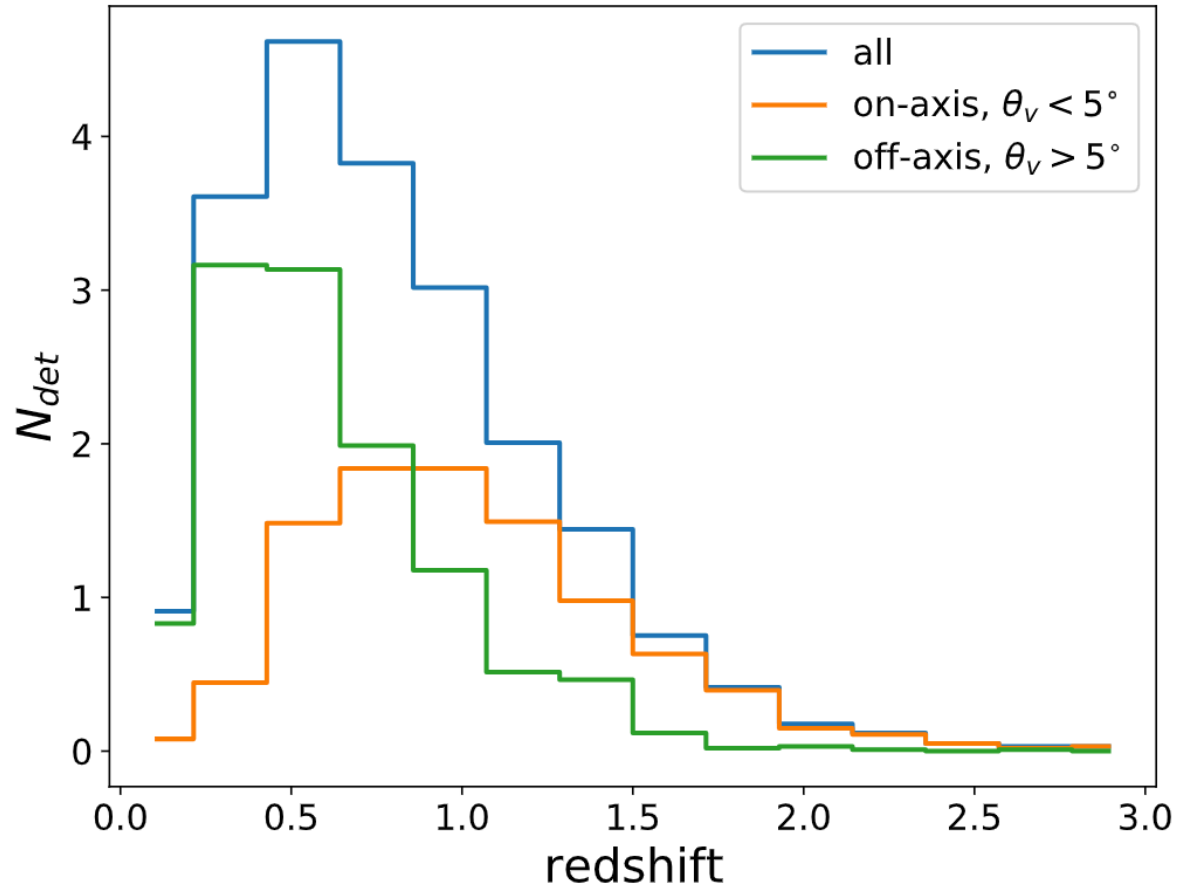
Instrument	$\Delta 10$	$\Delta 15$	2L 15	2L 20
THESEUS-SXI survey	10^{+3}_{-2}	13^{+3}_{-4}	12^{+3}_{-3}	12^{+3}_{-3}
THESEUS-(SXI+XGIS) survey	21^{+6}_{-7}	21^{+8}_{-6}	20^{+7}_{-5}	21^{+7}_{-7}

HF sensitivity detectors

Instrument	$\Delta 10$	$\Delta 15$	2L 15	2L 20
THESEUS-SXI survey	8^{+2}_{-3}	11^{+2}_{-4}	10^{+2}_{-3}	11^{+2}_{-2}
THESEUS-(SXI+XGIS) survey	16^{+6}_{-5}	19^{+8}_{-5}	19^{+4}_{-5}	21^{+8}_{-6}

- number of joint detections is around 10 for SXI (20 for SXI+XGIS) per year independently of the arms lengths and the geometries
- number remains almost the same also without accessing low-frequencies

Joint GW+afterglow detections per year



THESEUS

THESEUS-(SXI+XGIS) operating with
2L20km full sensitivity

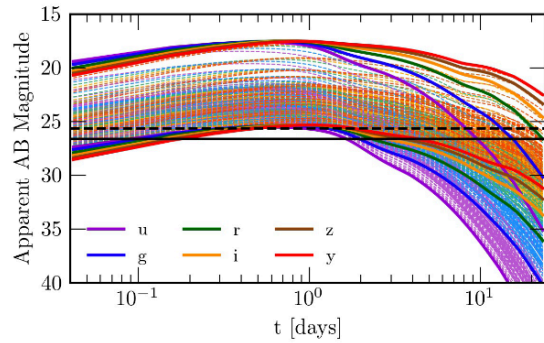
- The majority of the joint detections are within $z = 1$
- The majority of the afterglows are detectable up to a redshift where there is no significant difference among the GW detection efficiency

THERMAL EMISSION - KILONOVAE

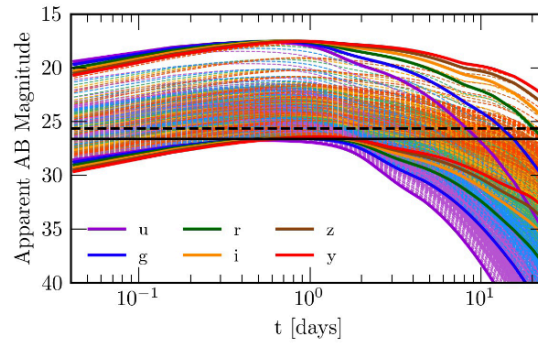
KILONOVA PHYSICS, NUCLEOSYNTHESIS,
NUCLEAR PHYSICS and COSMOLOGY

ET+Vera Rubin synergy

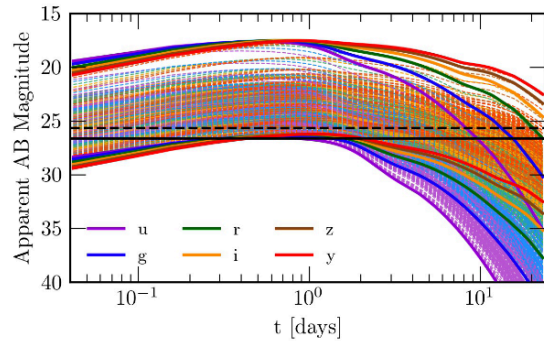
BNSs detected with a sky-localization < 40 deg²



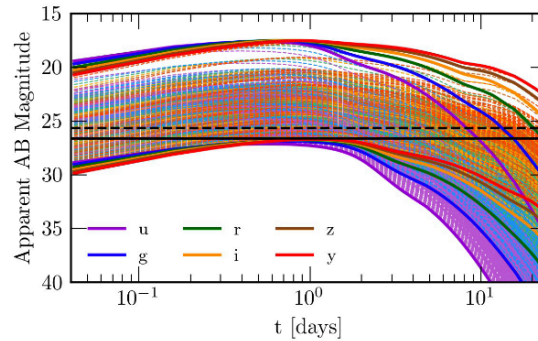
(a) Δ 10 km HFLF cryo



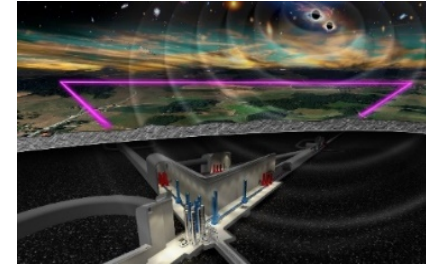
(b) Δ 15 km HFLF cryo



(c) 2L 15 km HFLF cryo



(d) 2L 20 km HFLF cryo



VERA RUBIN OBSERVATORY ToO:

- Follow-up of events localized better than 20, 40 and 100 sq. degrees
- 600s (1800 s) observations the first and second nights after the merger in two filters (g and i)

ET+Vera Rubin synergy

Full (HFLF cryo) sensitivity detectors

Configuration	$N_{\text{GW,VRO}}$ $\Omega < 20 \text{ deg}^2$	VRO time	$N_{\text{GW,VRO}}$ $\Omega < 40 \text{ deg}^2$	VRO time	$N_{\text{GW,VRO}}$ $\Omega < 100 \text{ deg}^2$	VRO time
$\Delta 10$	14 (14)	1.1% (3.3%)	36 (39)	5.1% (15%)	96	40%
$\Delta 15$	38 (42)	3.3% (9.8%)	84 (101)	14.2% (42%)	163	> 100%
2L 15	28 (28)	2.2% (6.5%)	62 (77)	10.6% (31%)	189	93%
2L 20	55 (64)	5% (14.9%)	115 (152)	23.1% (68%)	324	> 100%

  
600 s 1800 s Percentage of
VRO time

 Increase number of detections but the percentage of time to be used becomes prohibitive and more contaminants!

- 2L20km misaligned configuration is the best enabling to detect between several tens and a few hundreds of kilonova counterparts
- $\Delta 15$ km is slightly better than 2L15km giving a number of detection about 30% larger
- $\Delta 15$ km is significantly better than $\Delta 10$ km giving about a factor 2 larger number of detections

ET+Vera Rubin synergy

Full (HFLF cryo) sensitivity detectors

Configuration	$N_{\text{GW,VRO}}$ $\Omega < 20 \text{ deg}^2$	VRO time	$N_{\text{GW,VRO}}$ $\Omega < 40 \text{ deg}^2$	VRO time	$N_{\text{GW,VRO}}$ $\Omega < 100 \text{ deg}^2$	VRO time
$\Delta 10$	14 (14)	1.1% (3.3%)	36 (39)	5.1% (15%)	96	40%
$\Delta 15$	38 (42)	3.3% (9.8%)	84 (101)	14.2% (42%)	163	> 100%
2L 15	28 (28)	2.2% (6.5%)	62 (77)	10.6% (30%)	89	93%
2L 20	55 (64)	5% (14.9%)	115 (150)	19.8% (57%)	24	> 100%

Without low-frequency

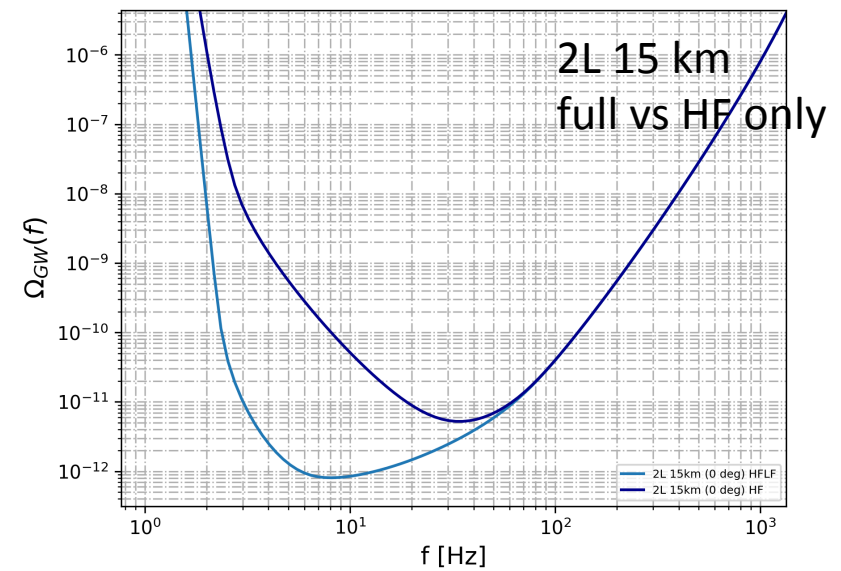
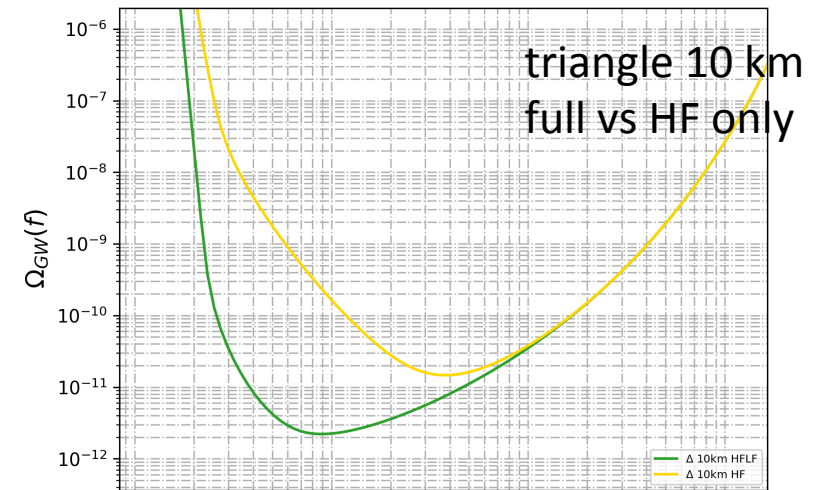
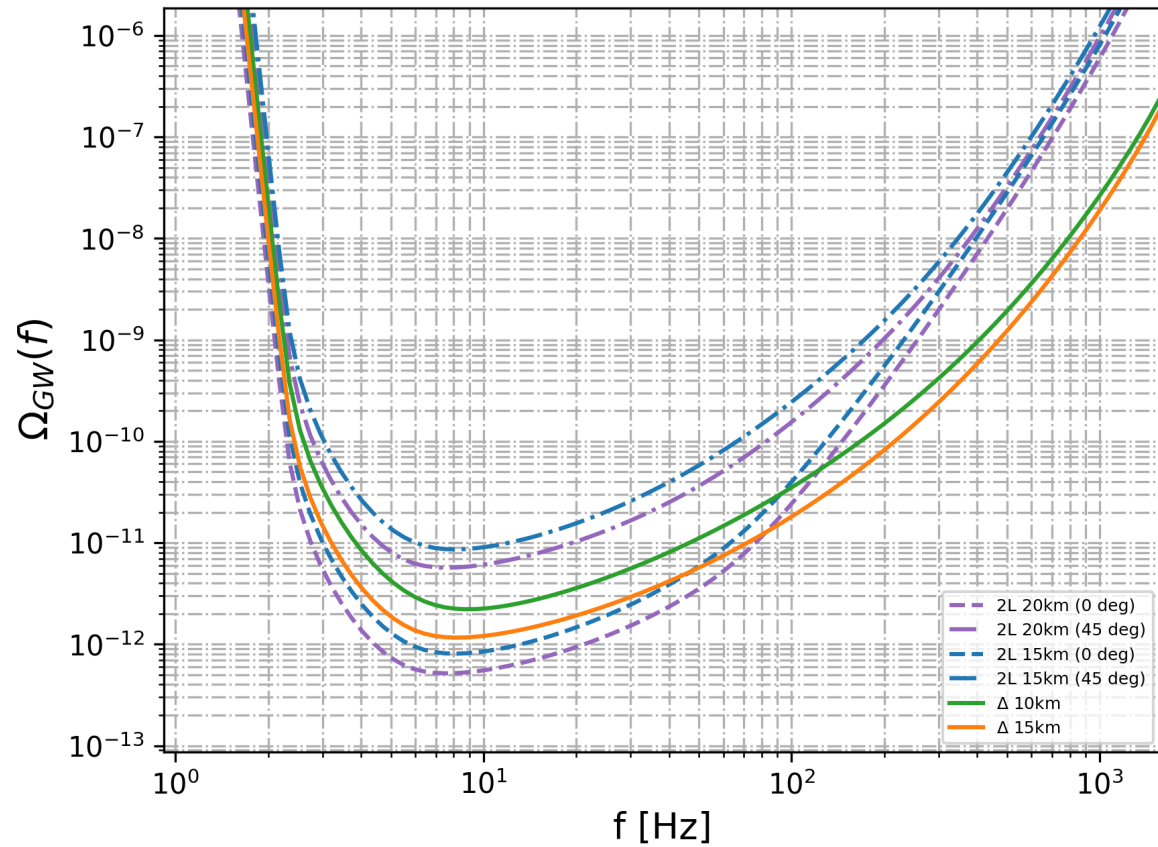
The presence of low-frequency is critical to detect a large number of kilonovae counterparts

Configuration	$N_{\text{GW,VRO}}$ $\Omega < 20 \text{ deg}^2$	VRO time	$N_{\text{GW,VRO}}$ $\Omega < 40 \text{ deg}^2$	VRO time	$N_{\text{GW,VRO}}$ $\Omega < 100 \text{ deg}^2$	VRO time
$\Delta 10$	0 (0)	0% (0%)	2 (2)	0.3% (0.8%)	4	2%
$\Delta 15$	2 (2)	0.2% (0.5%)	3 (4)	0.7% (1.9%)	8	7.5%
2L 15	3 (4)	0.4% (1.2%)	7 (7)	1.3% (3.9%)	26	11%
2L 20	5 (4)	0.6% (1.6%)	15 (18)	3.1% (9.3%)	32	20.8%

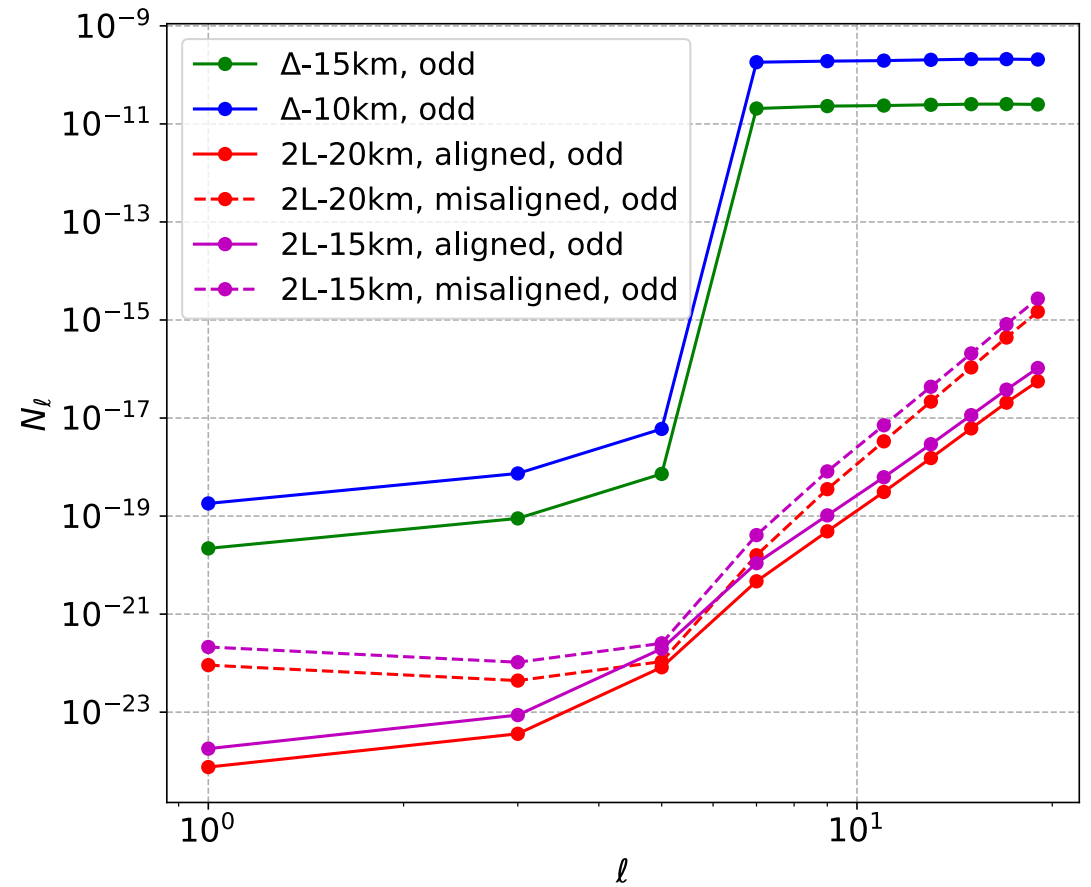
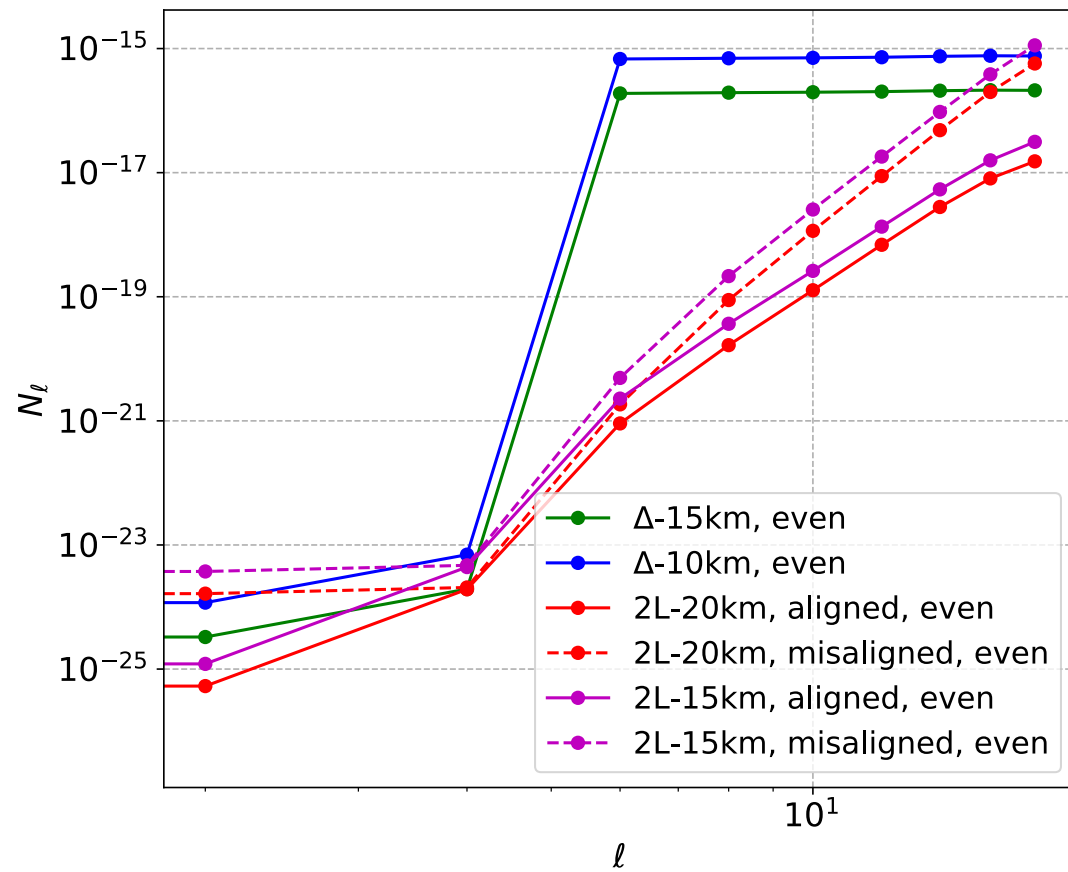
ONLY HF:

- small number (a few) of detections per year expected with the Δ -HF configurations
- this number increases to a few tens for the 2L-HF configurations

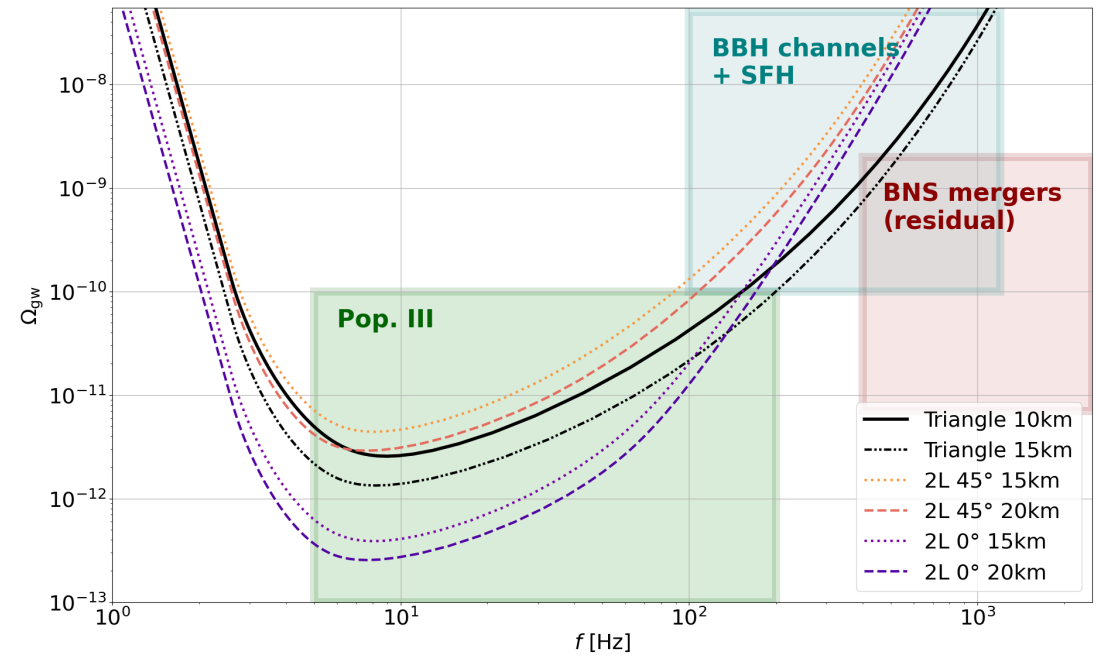
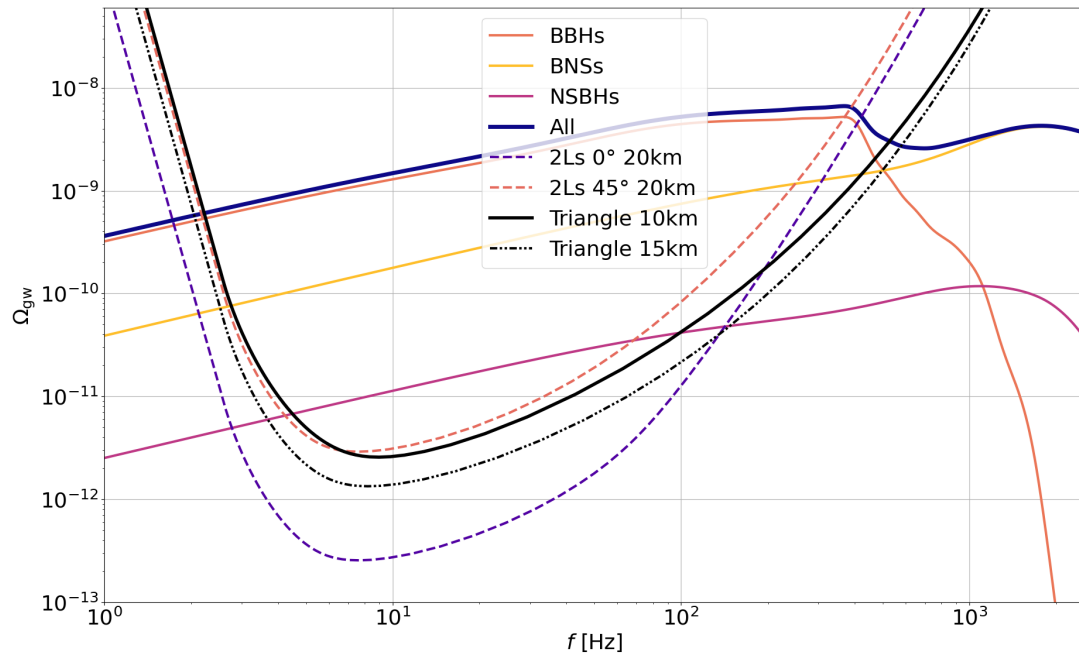
stochastic backgrounds



multipole decomposition of the stochastic background



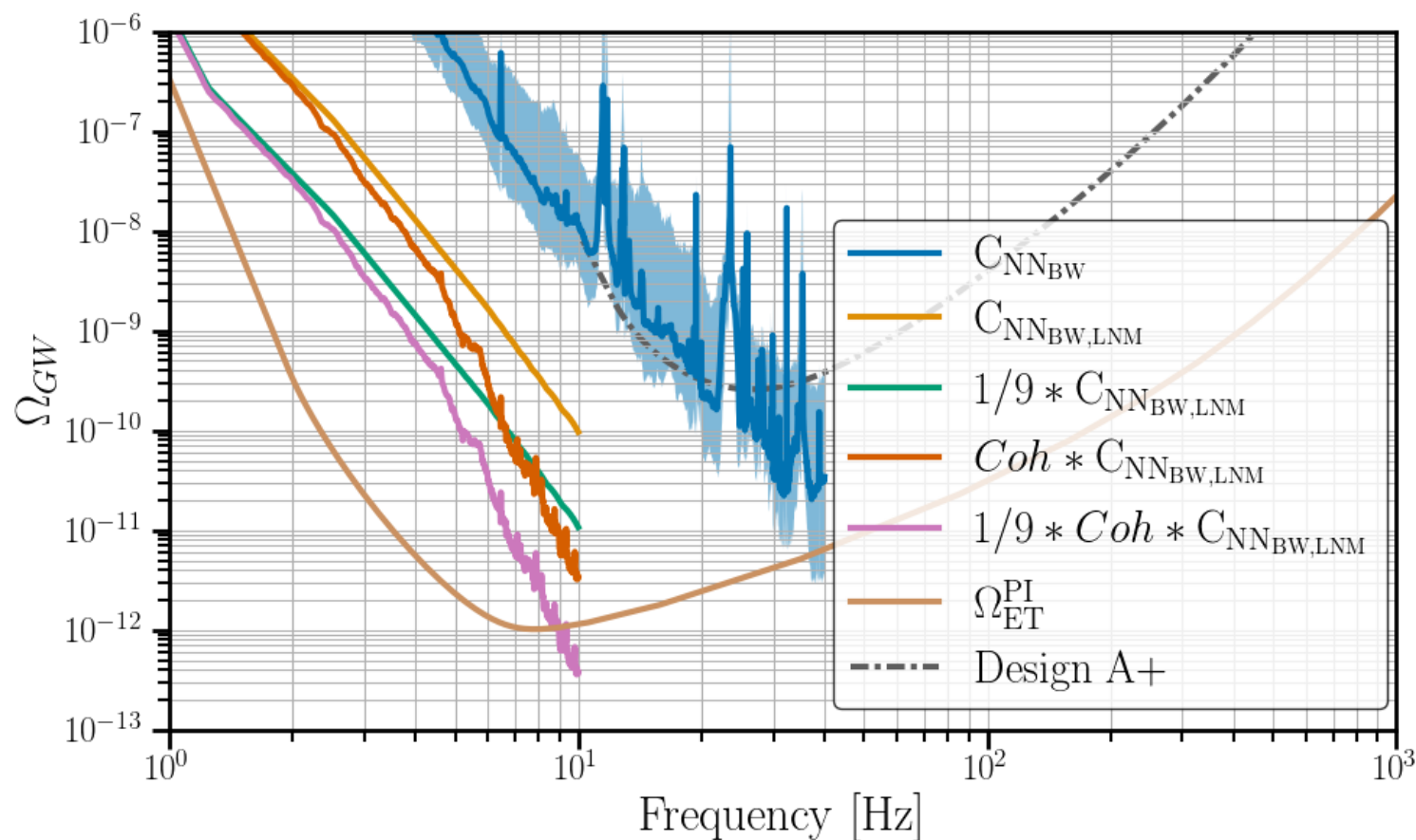
astrophysical signatures in stochastic bkgd



signatures imprinted in deviations from $f^{2/3}$

correlated Newtonian, seismic and magnetic noise.

A threat for the triangle?



impacts stochastic
backgrounds searches
but possibly also CBC
and unmodeled bursts

See talk by
Kamiel Janssens

Impacts on specific science cases

(a selection of the examples worked out)

Physics near BH horizon

$\text{SNR}_{\text{GW150914}}$	HFLF-cryo	HF-only
Δ -10 km	141	141
Δ -15 km	190	190
2L-15 km-0°	196	196
2L-15 km-45°	192	192
2L-20 km-0°	240	240
2L-20 km-45°	235	235

Ringdown SNR of GW150914-like event

$$\frac{\Delta f_{220}}{f_{220}} \sim 0.2\% \left(\frac{100}{\text{SNR}} \right), \quad \frac{\Delta \tau_{220}}{\tau_{220}} \sim 2\% \left(\frac{100}{\text{SNR}} \right)$$

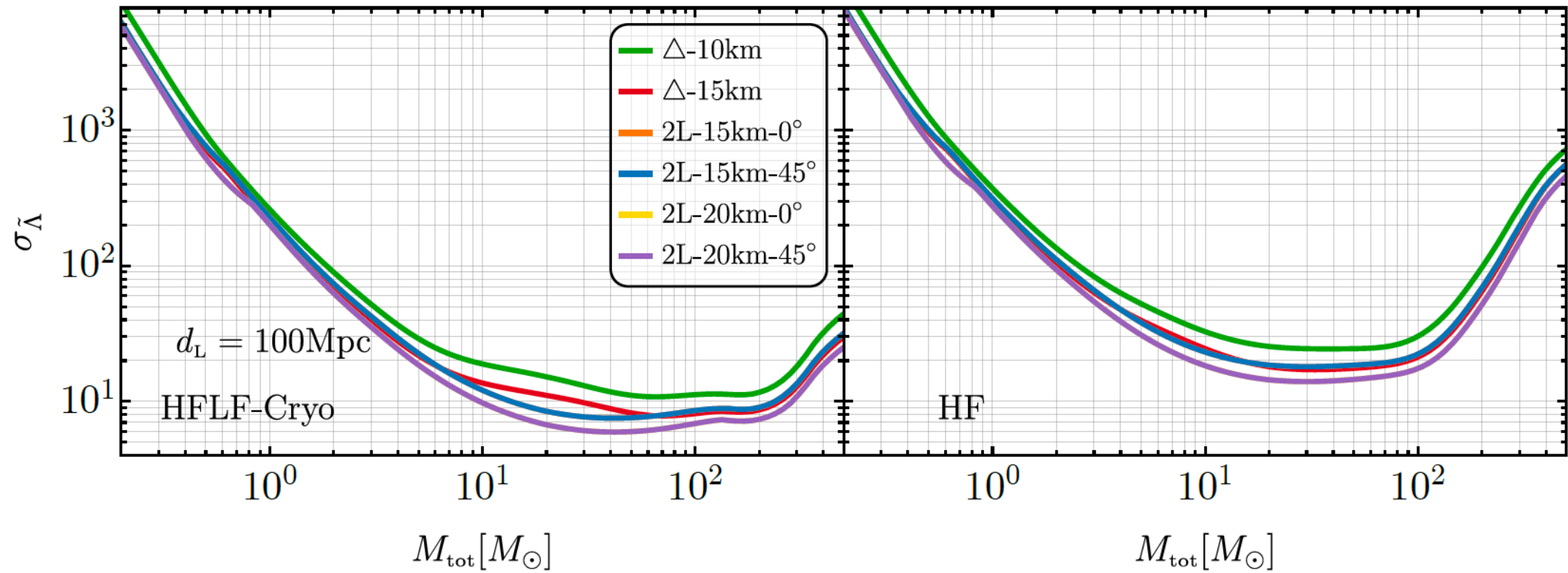
	$N_{\text{det}}(\text{SNR} \geq 12)$	$N_{\text{det}}(\text{SNR} \geq 50)$	$N_{\text{det}}(\text{SNR} \geq 100)$	max(SNR)
LVKI-O5	22	0	0	34
ET				
Δ -10 km	5272	41	4	255
Δ -15 km	12916	139	15	312
2L-15 km-0°	11602	109	11	265
2L-15 km-45°	11277	110	10	323
2L-20 km-0°	19081	248	22	309
2L-20 km-45°	18695	252	21	376

Ringdown detections per year

ET (+1CE)	$N_{\text{det}}(\text{SNR} \geq 12)$	$N_{\text{det}}(\text{SNR} \geq 50)$	$N_{\text{det}}(\text{SNR} \geq 100)$	max(SNR)
Δ -10 km	17690	202	17	296
Δ -15 km	24495	335	32	346
2L-15 km-0°	23202	311	29	304
2L-15 km-45°	23125	308	30	356
2L-20 km-0°	29278	490	45	343
2L-20 km-45°	29298	482	42	405
ET (+2CE)				
Δ -10 km	22056	290	26	302
Δ -15 km	28498	424	40	351
2L-15 km-0°	27146	408	39	311
2L-15 km-45°	27134	396	38	362
2L-20 km-0°	32796	606	54	348
2L-20 km-45°	33006	593	53	409

Differences remain significant also with 1 or 2 CE

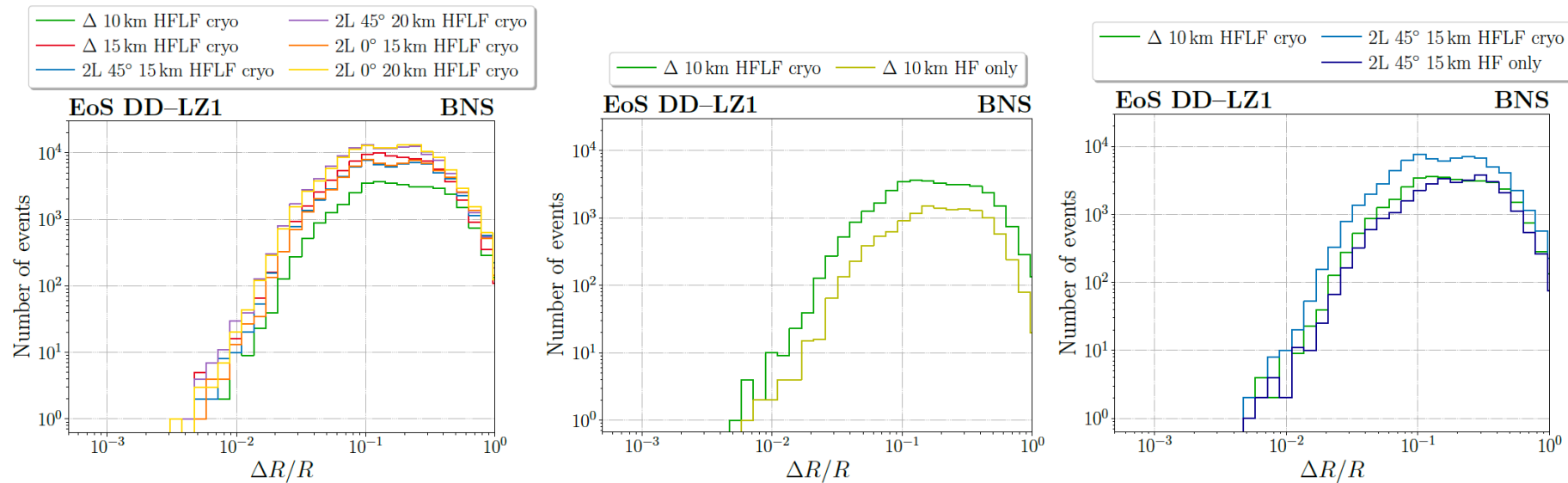
distinguishing exotic compact objects from BHs



Nuclear Physics

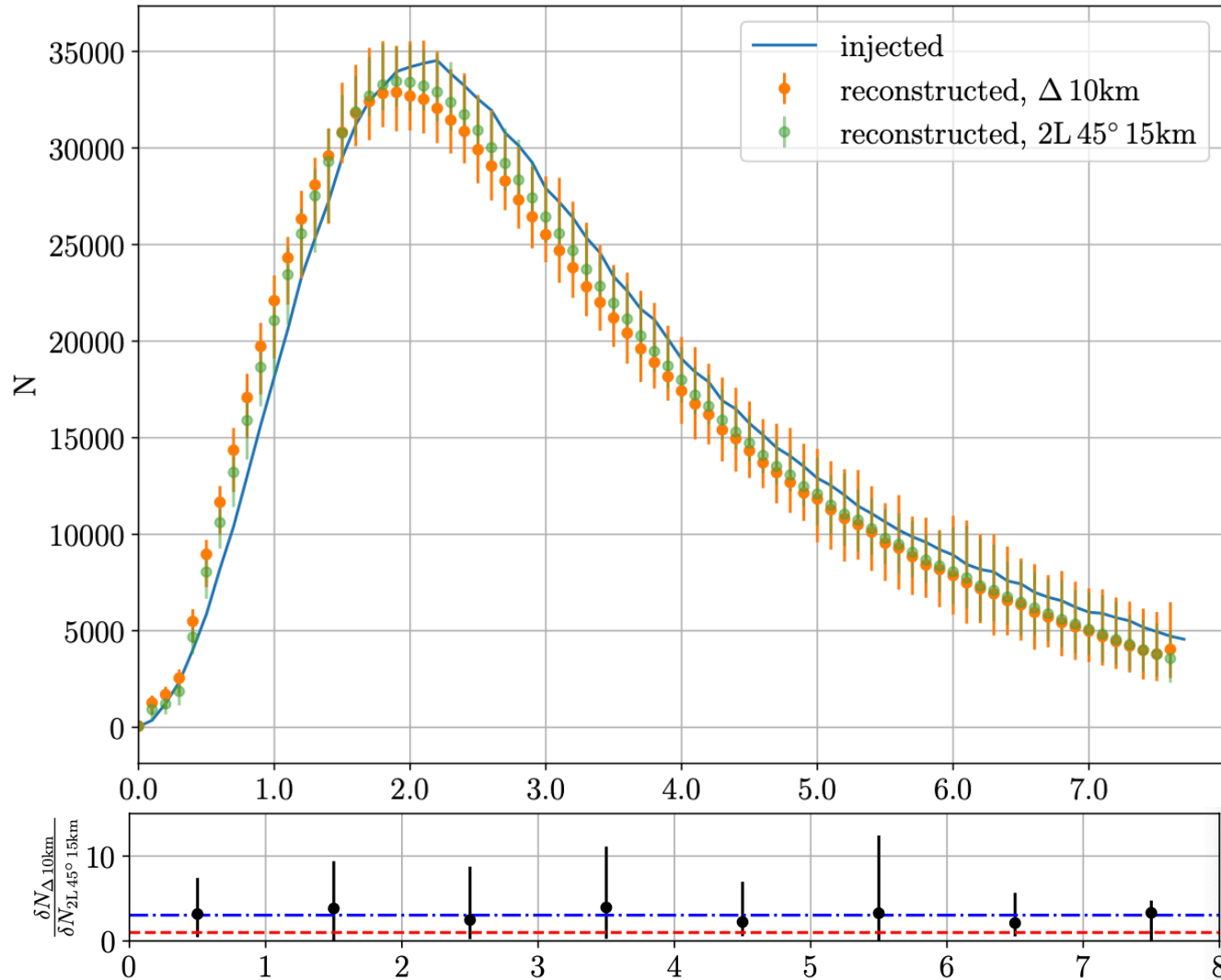
- see talk by Tim Dietrich

one example:



2L-15 HF only as good as full 10km triangle

Population studies



Merger rate reconstruction

2L-15km both 10km triangle and
2L-15km- 45° reconstruct it correctly,
but m- 45° is better by a factor 2-3

primordial BHs

Detections at $z > 30$ are a smoking-gun signature

Configuration	$N_{\text{det}}(z > 10)$ [1/yr]	$N_{\text{det}}(z > 30)$ [1/yr]	$f_{\text{PBH}}^{\text{constrained}} [\times 10^{-5}]$
Δ -10km	1140.01	76.81	2.61
Δ -15km	1763.87	260.65	1.42
2L-15km-0°	1596.61	238.16	1.48
2L-15km-45°	1650.87	220.86	1.54
2L-20km-0°	1983.97	433.82	1.10
2L-20km-45°	2080.13	415.80	1.12

(based on a PBH population model fitted to GWTC-3)

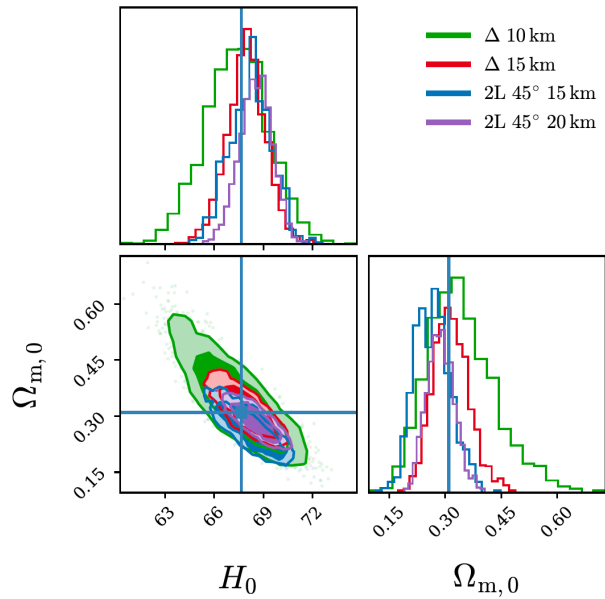
LF crucial: $N(z > 30) = 0$ otherwise !

significant differences
also in a network with 1CE

Configuration	$N_{\text{det}}(z > 10)$ [1/yr]	$N_{\text{det}}(z > 30)$ [1/yr]	$f_{\text{PBH}}^{\text{constrained}} [\times 10^{-5}]$
CE40km	1373.48	47.07	3.34
Δ-10km + CE40km	1940.35	180.08	1.71
Δ -15km + CE40km	2275.96	372.14	1.19
2L-15km-45° + CE40km	2210.49	332.89	1.26
2L-20km-45° + CE40km	2476.43	522.32	1.00

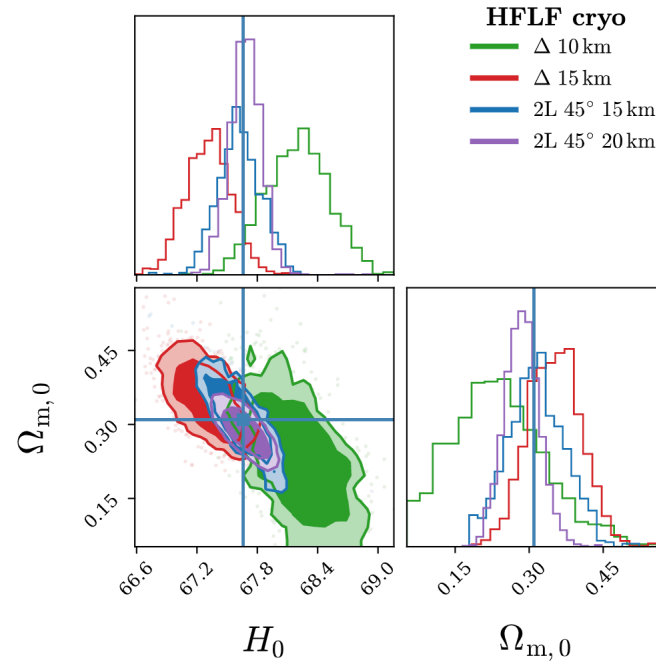
Cosmology

Joint GW-GRB detections, ET+THESEUS



Configuration	$\Delta H_0/H_0$	$\Delta\Omega_M/\Omega_M$
Δ -10km	0.057	0.546
Δ -15km	0.035	0.290
2L-15km-45°	0.040	0.370
2L-20km-45°	0.029	0.276

Joint GW-kilonova detections, ET+VRO



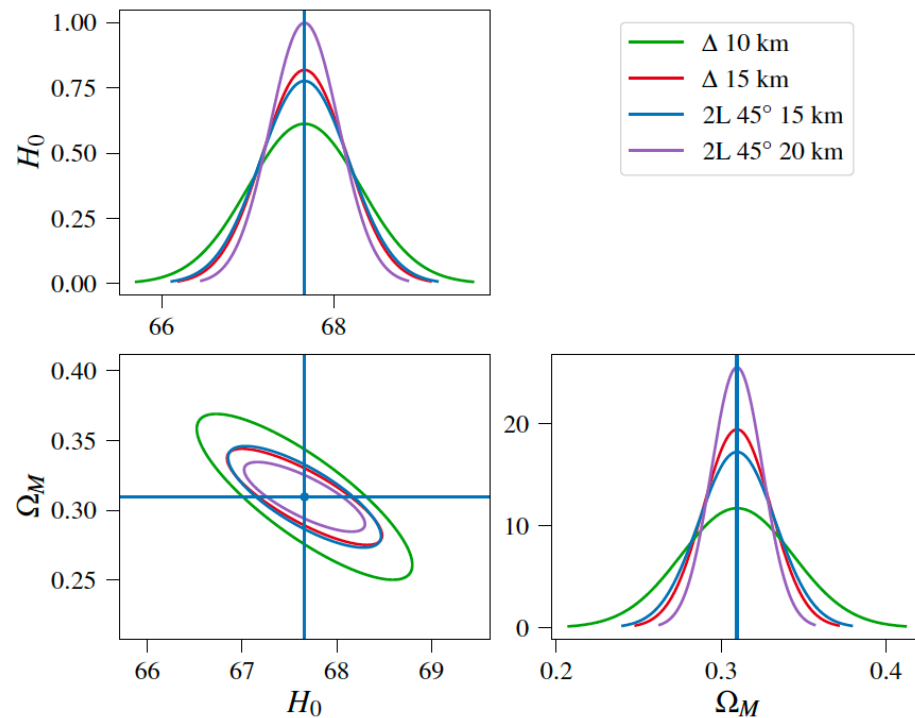
HFLF cryogenic		
Configuration	$\Delta H_0/H_0$	$\Delta\Omega_M/\Omega_M$
Δ -10km	0.009	0.832
Δ -15km	0.007	0.303
2L-15km-45°	0.006	0.370
2L-20km-45°	0.004	0.243

HF only		
Configuration	$\Delta H_0/H_0$	$\Delta\Omega_M/\Omega_M$
Δ -10km	0.065	1.23
Δ -15km	0.057	1.86
2L-15km-45°	0.066	1.31
2L-20km-45°	0.031	1.22

Note: the bounds becomes stronger using the Planck prior on Ω_M

See the paper for DE EoS and modified GW propagation

NS source-frame mass (and then z) determined from tidal deformability of NS



Configuration	$\Delta H_0/H_0$	$\Delta \Omega_M/\Omega_M$
Δ -10km	9.63×10^{-3}	1.10×10^{-1}
Δ -15km	7.20×10^{-3}	6.62×10^{-2}
2L-15km-45°	7.59×10^{-3}	7.47×10^{-2}
2L-20km-45°	5.90×10^{-3}	5.04×10^{-2}

Summing up....

Comparison between geometries

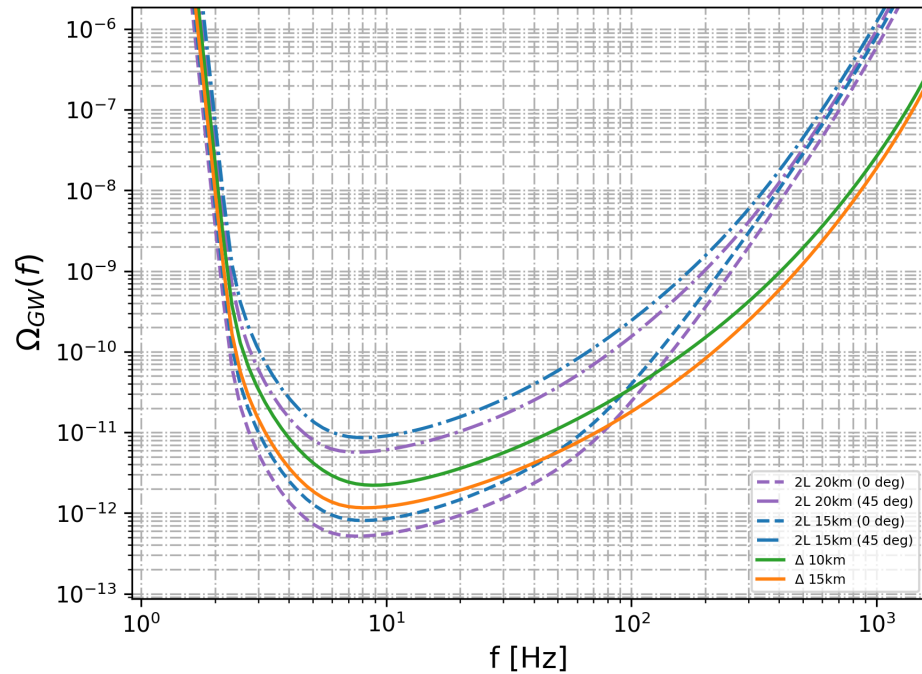
- for BBH parameter estimation:
 - the 2L-15km-45° improves significantly on the 10 km triangle for d_L and angular localization, and is slightly better (~ 2) for the other parameters,
 - is equal or better even than the 15 km triangle
 - in a network with 1 or 2CE the differences are still significant
- for BNS, the effect is even larger

Configuration	$\Delta d_L/d_L \leq 0.3$	$\Delta d_L/d_L \leq 0.1$	$\Delta \Omega_{90\%} \leq 100 \text{ deg}^2$	$\Delta \Omega_{90\%} \leq 10 \text{ deg}^2$
Δ -10km-HFLF-Cryo	748	52	184	8
Δ -15km-HFLF-Cryo	1756	153	479	23
2L-15km-45°-HFLF-Cryo	4328	479	559	25
2L-20km-45°-HFLF-Cryo	7821	919	1028	43
2L-15km-0°-HFLF-Cryo	774	48	293	12
2L-20km-0°-HFLF-Cryo	1499	104	565	23

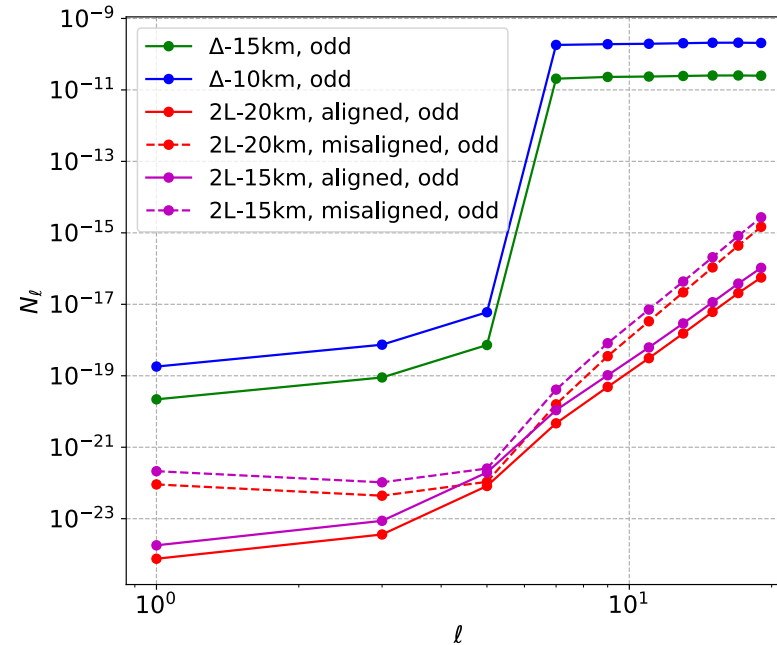
For multi-messenger astronomy:

- $2L_{15km_{45^\circ}}$ better than 10 km triangle (and comparable to 15 km triangle) enabling observation of a larger number of well-localized events up to a larger redshift
- number of short GRBs with an associated GW signal increases by about 30%, and the number of expected kilonovae counterparts increases by a factor of 2
- for pre-merger alerts, the 15 km triangle is performing better than the 10 km triangle and the $2L_{15km_{45^\circ}}$, reaching almost the capability of the $2L_{20km}$ configuration

- for stochastic backgrounds

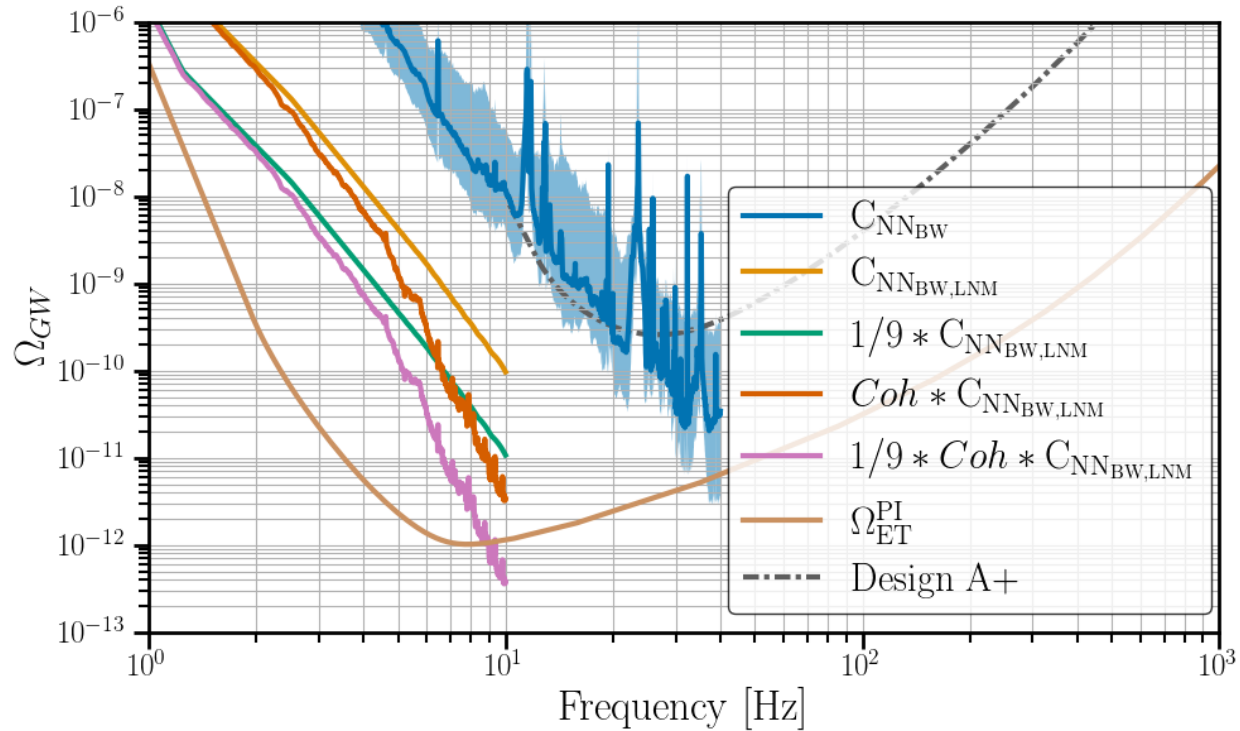


for the isotropic sensitivity:
 2L at 45° the less good
 2L parallel the best below 100 Hz
 triangle the best above 100Hz



For angular resolution:
 2L better than triangle

- correlated Newtonian and seismic noise



a potential treath for the triangle

also, correlated magnetic noise
and lightening strikes

individual science case typically show an improvement by a factor 2-3 from the 10km triangle to 2L-15km-45°

- tests of GR:

SNR _{GW150914}	HFLF-cryo
Δ-10 km	141
Δ-15 km	190
2L-15 km-0°	196
2L-15 km-45°	192

	$N_{\text{det}}(\text{SNR} \geq 12)$	$N_{\text{det}}(\text{SNR} \geq 50)$	$N_{\text{det}}(\text{SNR} \geq 100)$	max(SNR)
LVKI-O5	22	0	0	34
ET				
Δ-10 km	5272	41	4	255
Δ-15 km	12916	139	15	312
2L-15 km-0°	11602	109	11	265
2L-15 km-45°	11277	110	10	323

- nuclear physics: minor differences (ΔR from 10.0m to 6.4m)

- merger rate reconstruction; improvement by a factor ~3

- PBH: improvement by a factor ~3 for events at $z > 30$

- cosmology: improvements ~1.5 on H_0 , w_0 , Ξ_0

In general, results for 2L-15km-45° quite comparable to 15-km triangle

Conclusions on the geometries

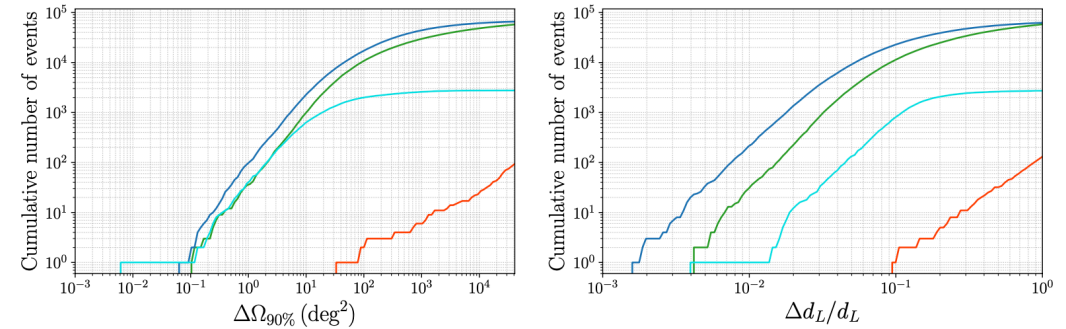
1. All the triangular and 2L geometries that we have investigated can be the baseline for a superb 3G detector, that will allow us to improve by orders of magnitudes compared to 2G detectors, and allow us to penetrate deeply into unknown territories.

2a. The 2L-15km-45° configuration in general offers better scientific return with respect to the 10 km triangle, improving on most figures of merits and scientific cases, by factors typically of order 2-3 on the errors of the relevant parameters.

2b. The 2L-15km-45° configuration has a scientific output very similar to that of the 15 km triangle

- a single L shaped detectors, even if 20km or more, not inserted in a 3G network, is not a viable solution

- (comparatively) very poor angular localization and measurement of d_L
 \Rightarrow total loss of MMO, cosmology, ...



- no stochastic backgrounds
- difficult to distinguish short signals from glitches

3. A single L-shaped detector is not a viable alternative, independently of arm length. If a single site solution should be preferred for ET, the detector must necessarily have the triangular geometry.

The role of the LF instrument

For BNS, catastrophic degradation on sky localization and luminosity distance (LF allows BNS to stay a longtime in the bandwidth)

Configuration	$\Delta d_L/d_L \leq 0.3$	$\Delta d_L/d_L \leq 0.1$	$\Delta\Omega_{90\%} \leq 100 \text{ deg}^2$	$\Delta\Omega_{90\%} \leq 10 \text{ deg}^2$
Δ -10km-HFLF-Cryo	748	52	184	8
Δ -15km-HFLF-Cryo	1756	153	479	23
2L-15km-45°-HFLF-Cryo	4328	479	559	25
2L-20km-45°-HFLF-Cryo	7821	919	1028	43
2L-15km-0°-HFLF-Cryo	774	48	293	12
2L-20km-0°-HFLF-Cryo	1499	104	565	23
Δ -10km-HF	4	1	4	0
Δ -15km-HF	7	1	11	1
2L-15km-45°-HF	126	12	11	0
2L-20km-45°-HF	262	22	24	1
2L-15km-0°-HF	20	1	11	1
2L-20km-0°-HF	28	2	24	1

⇒ no MMO, no standard sirens cosmology

- premerger alerts impossible without the LF instrument

Full (HFLF cryo) sensitivity detectors

Configuration	$\Delta\Omega_{90\%}$	All orientation BNSs			BNSs with $\Theta_v < 15^\circ$		
	[deg ²]	30 min	10 min	1 min	30 min	10 min	1 min
$\Delta 10\text{km}$	10	0	1	5	0	0	0
	100	10	39	113	2	8	20
	1000	85	293	819	10	34	10
	All detected	905	4343	23597	81	393	2312

HF sensitivity detectors

Configuration	$\Delta\Omega_{90\%}$	All orientation BNSs			BNSs with $\Theta_v < 15^\circ$		
	[deg ²]	30 min	10 min	1 min	30 min	10 min	1 min
$\Delta 10\text{km}$	100	0	0	0	0	0	0
	1000	0	0	4	0	0	1
	All detected	0	3	317	0	0	26

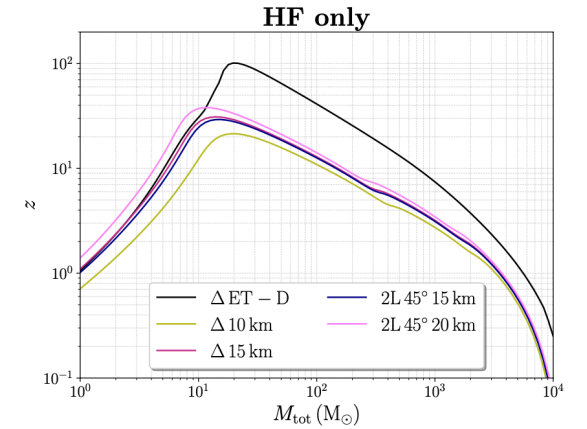
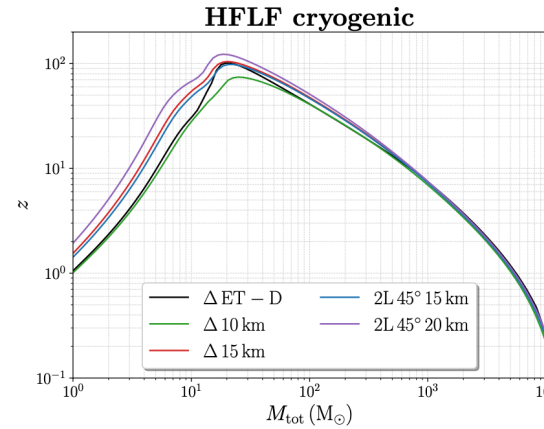
2L 15 km misaligned	10	0	1	8	0	0	0
	100	20	54	169	2	7	26
	1000	194	565	1399	23	73	199
	All detected	2172	9598	39499	198	863	3432

2L 15 km misaligned	100	0	0	0	0	0	0
	1000	0	0	7	0	0	3
	All detected	0	7	743	0	1	69

dramatic impact on the possibility of detecting precursor and probe prompt/early counterpart \Rightarrow miss the info on GRB engine, jet launch, kilonova ejecta

- joint GW-GRB detections decrease by 40% (10km triangle) or 30% (2L-15km)

- HF only has a significantly smaller reach in distance



- for BNS: from $z \approx 4$ to $z \approx 4$ (triangle 10km) or from $z \approx 6$ to $z \approx 3$ (2L-15km) misses the peak of the star formation rate
- for PBH: impossible to identify them on the basis of $z > 30$

Configuration	$N_{\text{det}}(z > 10)$ [1/yr]	$N_{\text{det}}(z > 30)$ [1/yr]	$f_{\text{PBH}}^{\text{constrained}} [\times 10^{-5}]$
Δ -10km	1140.01	76.81	2.61
Δ -15km	1763.87	260.65	1.42
2L-15km-0°	1596.61	238.16	1.48
2L-15km-45°	1650.87	220.86	1.54
2L-20km-0°	1983.97	433.82	1.10
2L-20km-45°	2080.13	415.80	1.12

Configuration	$N_{\text{det}}(z > 10)$ [1/yr]	$N_{\text{det}}(z > 30)$ [1/yr]	$f_{\text{PBH}}^{\text{constrained}} [\times 10^{-5}]$
Δ -10km-HF	15.47	0.00	-
Δ -15km-HF	84.91	0.00	-
2L-15km-0°-HF	75.08	0.00	-
2L-15km-45°-HF	69.48	0.00	-
2L-20km-0°-HF	177.84	0.00	-
2L-20km-45°-HF	169.81	0.00	-

- IMBH: reduction by a factor ~ 5 in comoving volume explored

- for many other aspects of the science case, the loss of the LF instrument is not as disruptive, but still means a reduction by by a factor 2-3 in accuracy on relevant parameters

Therefore:

4. The low-frequency sensitivity is crucial for exploiting the full scientific potential of ET. In the HF-only configuration, independently of the geometry chosen, several crucial scientific targets of the science case would be lost or significantly diminished.

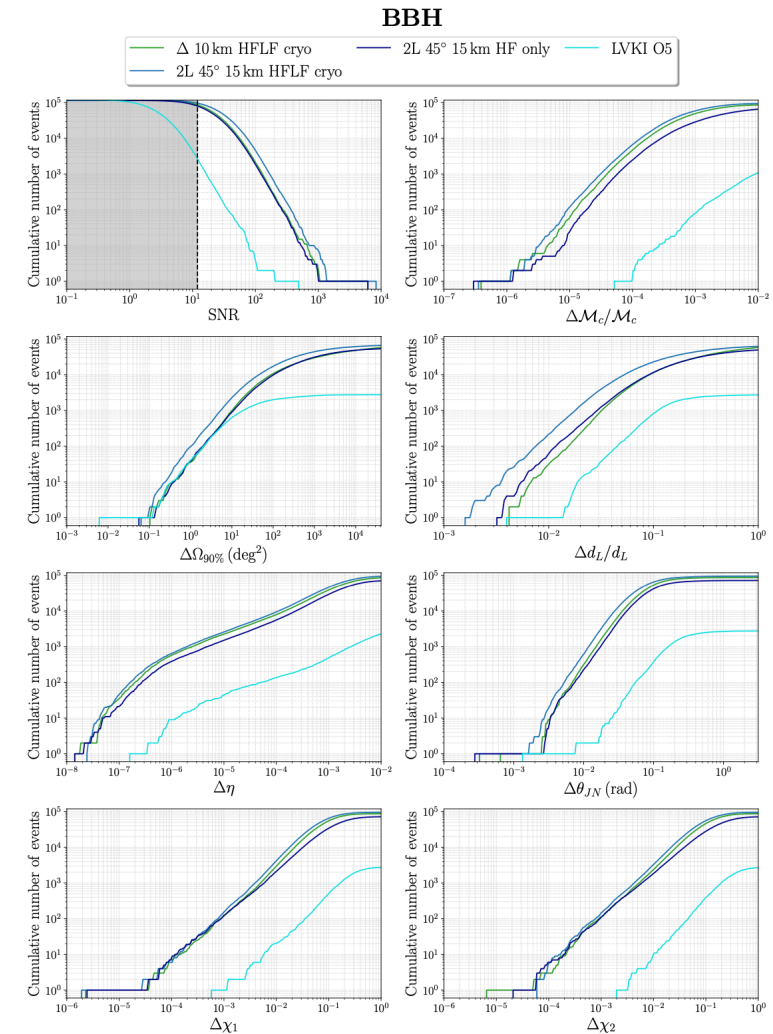
There are, however, very interesting specific targets insensitive to LF and can be fully reached with HF-only

- in MMO, joint GW+X-ray afterglow(THESEUS) detections and (partly) GW+GRB
- cosmological stochastic backgrounds with a 'blue' spectrum
- tests of physics near the BH horizon
- post-merger signal of BNS
- search for sub-solar mass PBHs

5. There are some very interesting targets of the Science Case that depend only on the HF sensitivity, and that could be fully reached with an HF-only instrument.

In certain cases, the 2L-15km-45° HF-only is comparable to the 10km triangle with full HFLF-cryo sensitivity

- parameter estimation of BBHs (but not BNS!)
- nuclear physics
- all items where the LF instrument is not important, see above



Summary of the summary....

1. All the triangular and 2L geometries that we have investigated can be the baseline for a superb 3G detector, that will allow us to improve by orders of magnitudes compared to 2G detectors, and allow us to penetrate deeply into unknown territories.

2a. The 2L-15km-45° configuration in general offers better scientific return with respect to the 10 km triangle, improving on most figures of merits and scientific cases, by factors typically of order 2-3 on the errors of the relevant parameters.

2b. The 2L-15km-45° configuration has a scientific output very similar to that of the 15 km triangle

3. A single L-shaped detector is not a viable alternative, independently of arm length. If a single site solution should be preferred for ET, the detector must necessarily have the triangular geometry.

4. *The low-frequency sensitivity is crucial for exploiting the full scientific potential of ET. In the HF-only configuration, independently of the geometry chosen, several crucial scientific targets of the science case would be lost or significantly diminished.*

5. *There are some very interesting targets of the Science Case that depend only on the HF sensitivity, and that could be fully reached with an HF-only instrument.*

6. *For several important aspects of the Science Case, the 2L with 15 km arms at 45° , already in the HF-only configuration, is comparable the 10 km triangle in a full HFLF-cryo configuration.*

Inputs for further studies

- The 2L-15km-45° appears to give a better possibility of going through staging:
 - commission first HF (already important results will be obtained)
 - move toward full HFLF-cryo sensitivity, maybe through intermediate HFLF-room sensitivity \Rightarrow input to the ISB
- start a detailed analysis of the costs of different configurations